Geol. Mag. **154** (2), 2017, pp. 334–353. © Cambridge University Press 2016
doi:10.1017/S0016756816000017

Integrated conodont biostratigraphy and carbon isotope chemostratigraphy in the Lower–Middle Ordovician of southern Sweden reveals a complete record of the MDICE

RONGCHANG WU*‡†, MIKAEL CALNER* & OLIVER LEHNERT§*¶

*Department of Geology, Lund University, Sölvegatan 12, SE-223 62 Lund, Sweden
‡Key Laboratory of Economic Stratigraphy and Palaeogeography, Nanjing Institute of Geology and Palaeontology, Chinese Academy of Sciences, 39 East Beijing Road, Nanjing 210008, China
§GeoZentrum Nordbayern, Lithosphere Dynamics, Friedrich-Alexander, University of Erlangen-Nürnberg, Schlossgarten 5, D-91054, Erlangen, Germany
¶Institute of Geology, Tallinn University of Technology, Ehitajate tee 5, Tallinn 19086, Estonia

(*Received* 17 March 2015; *accepted* 4 January 2016; *first published online* 22 February 2016)

Abstract – One of the few and most complete records of the MDICE (Middle Darriwilian Isotope Carbon Excursion) is herein documented from Baltoscandia. Based on a core section penetrating the condensed Lower–Middle Ordovician succession (~46 m) on the island of Öland, southeastern Sweden, we provide an integrated scheme for carbon isotope chemostratigraphy (313 samples) and conodont biostratigraphy (29 samples) for this period. The carbonate succession in the Tingskullen core records 12 conodont zones and 6 subzones, including the *Oepikodus evae*, *Trapezognathus diprion*, *Baltoniodus triangularis*, *B. navis*, *B. norrlandicus*, *Lenodus antivariabilis*, *L. variabilis*, *Yangtzeplacognathus crassus, Eoplacognathus pseudoplanus* (*Microzarkodina hagetiana* and *Microzarkodina ozarkodella* subzones), *E. suecicus*, *Pygodus serra* (*E. foliaceus*, *E. reclinatus, E. robustus* and *E. lindstroemi* subzones) and *Pygodus anserinus* zones in ascending order. The $\delta^{13}C_{carb}$ record reveals an apparently complete record of the MDICE, including a rising limb, a well-defined peak and a falling limb. The anomaly covers a thickness of *c*. 27 m in the core and spans the *Eoplacognathus pseudoplanus*, *E. suecicus*, *Pygodus serra* and *P. anserinus* conodont zones. Combined with the new, detailed conodont biostratigraphy, the MDICE in the Tingskullen core can be used for detailed correlation with successions from Baltica, North America, the Argentine Precordillera, South China and North China.

Keywords: carbon isotope stratigraphy, conodonts, biostratigraphy, Ordovician, Sweden.

1. Introduction

$\delta^{13}C$ chemostratigraphy has been accepted as a powerful tool for correlation of carbonate successions on a regional as well as global scale. A large number of studies focusing on the Ordovician Period have been published over the last ten years in order to clarify the framework of carbon isotope chemostratigraphy (Ludvigson *et al.* 1996, 2004; Patzkowsky *et al.* 1997; Ainsaar, Meidla & Martma, 1999; Brenchley *et al.* 2003; Buggisch, Keller & Lehnert, 2003; Saltzman, 2005; Saltzman & Young, 2005; Young, Saltzman & Bergström, 2005; Kaljo, Martma & Saadre, 2007; Bergström *et al.* 2009, 2012; Ainsaar *et al.* 2010; Azmy *et al.* 2010; Munnecke *et al.* 2011; Zhang *et al.* 2011). Based on previously published data, Bergström *et al.* (2009) compiled a composite $\delta^{13}C$ curve for the Ordovician showing six short-lived positive excursions from the Upper Ordovician, whereas only a single one was demonstrated from the Middle Ordovician and none from the Lower Ordovician. This is in part because relatively few studies have specifically dealt with Lower and Middle Ordovician strata. Recently, Albanesi *et al.* (2013) demonstrated that the MDICE (Middle Darriwilian Isotope Carbon Excursion) is present in the Precordillera of Argentina. Edwards & Saltzman (2014) documented two detailed $\delta^{13}C$ curves through the Lower–Middle Ordovician of the Great Basin, United States. In addition, Lehnert *et al.* (2014) named several small positive and negative carbon isotope excursions in the Lower and Middle Ordovician based on data from the Siljan district, Central Sweden, and from data previously published from Argentina (Buggisch, Keller & Lehnert, 2003). However, the global significance of some of these newly named excursions still needs to be verified.

In Baltoscandia, Ordovician $\delta^{13}C$ chemostratigraphy is especially well investigated in Estonia and Latvia (Ainsaar, Meidla & Tinn, 2004; Meidla *et al.* 2004; Ainsaar *et al.* 2007, 2010; Kaljo, Martma & Saadre, 2007). There are only a few studies from this area, however, that specifically focus on the Lower and Middle Ordovician. In Sweden, a thin suite of Ordovician strata is locally well exposed, including the very uniform so-called 'orthoceratite limestone' of Early and Middle Ordovician age (Jaanusson, 1976). Conodonts from these strata have been investigated in detail and many

†Author for correspondence: Rongchang.Wu@geol.lu.se; rcwu@nigpas.ac.cn

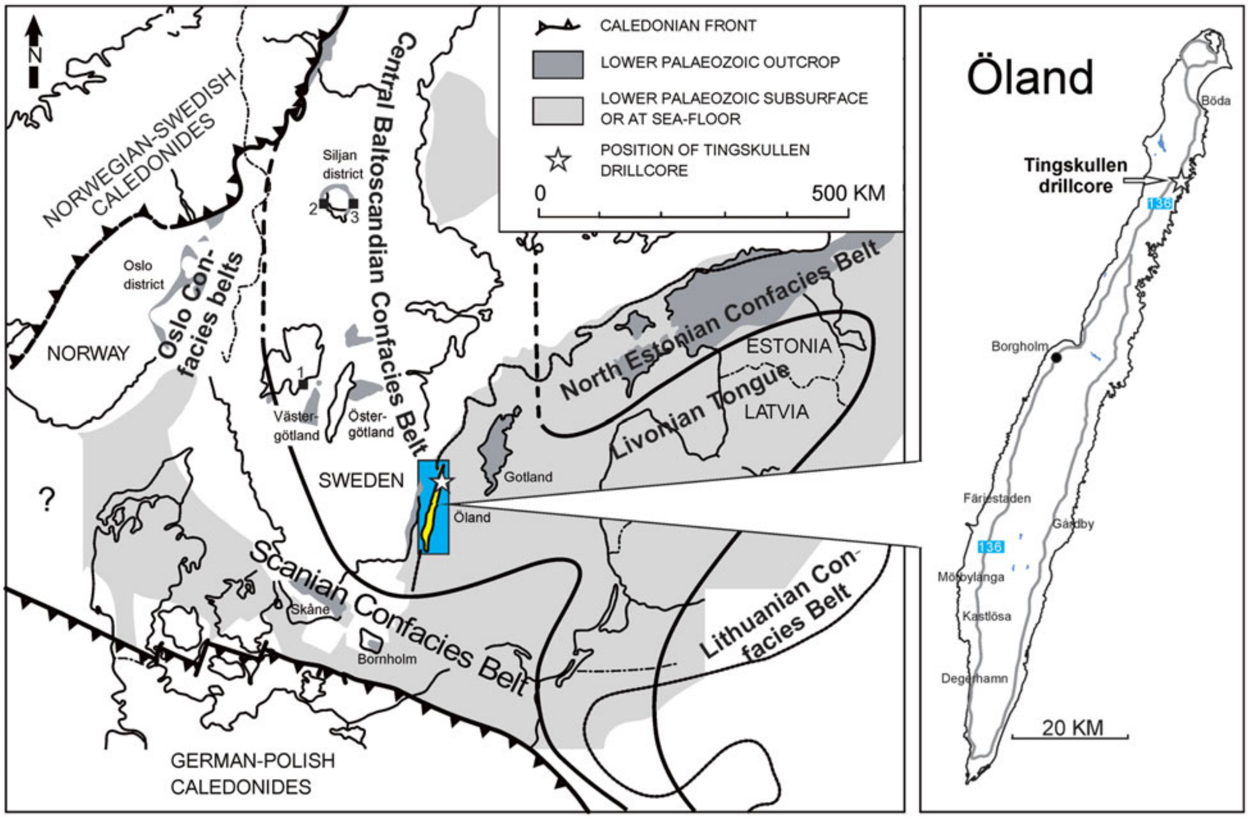

Figure 1. (Colour online) Ordovician palaeogeography of the Baltoscandian Basin modified from Pärnaste, Bergström & Zhou (2013) and Bergström, Pärnaste & Zhou (2013) showing the location of the Tingskullen drill core on Öland, southern Sweden and other Swedish core and outcrop sections mentioned in the text. 1 – Hällekis, Västergötland; 2 – Mora 001 core, Siljan district; 3 – Solberga 1 core, Siljan district.

studies have resulted in a standard conodont zonation for the Ordovician of Baltoscandia (e.g. Lindström, 1971; Bergström, 1971; Löfgren, 1994; Zhang, 1998*a*). Thus, the strata in Sweden provide an ideal record for integrating carbon isotope geochemistry with conodont biostratigraphy. In order to perform such studies in stratigraphically continuous sections, two drill cores have been recovered: one from the province of Östergötland in 2007 that covered the uppermost Middle Ordovician through Upper Ordovician, and one from the island of Öland in 2010 that covered the Lower–Middle Ordovician. These two cores together cover the entire Ordovician of southern Sweden, which in these areas is only a bit more than 100 m thick. The integrated carbon isotope chemostratigraphy and conodont biostratigraphy of the former core, representing the uppermost Middle Ordovician through Upper Ordovician, has been published recently by Bergström *et al.* (2011, 2012) and we will not comment more on this part of the succession. The latter core is the Tingskullen core that was drilled in 2010 in the northeastern part of the island of Öland. The first preliminary stratigraphic data from this core were published in conference proceedings by Calner *et al.* (2014). In this paper, we have expanded the original $\delta^{13}C$ dataset by more than 200 samples (Table 1) and, in addition, processed and analysed 29 conodont samples in order to add a detailed conodont biostratigraphy to the succession. We have also added plates showing the carbonate microfacies of the succession. The combined data help to put the Swedish Ordovician in a global context and add important data for global correlation of Lower–Middle Ordovician strata in general.

2. Geological setting and stratigraphy

During Middle–Late Ordovician times, the Baltic palaeoplate was situated between 60° and 30° S (Torsvik *et al.* 1992), moving towards the equator and covered by a shallow epicontinental sea. Based on lithofacies distribution and faunal composition in the Middle Ordovician, the sediments have been subdivided into three broad facies belts representing the Early through Middle Ordovician bathymetry of the basin (the confacies belts of Jaanusson, 1976, 1995; Fig. 1). The island of Öland in the Baltic Sea lies within the Central Baltoscandian Confacies Belt, where the Ordovician succession is largely composed of 'orthoceratite limestone', characterized by low sedimentary rates and numerous hardgrounds (Jaanusson, 1961).

The island of Öland is one of the classic areas for research on the Ordovician of Sweden. Limestone of Lower–Middle Ordovician age is distributed across the entire island with many natural exposures and abandoned as well as active quarries, especially along the western coastline of the island. Stouge (2004)

https://doi.org/10.1017/S0016756816000017 Published online by Cambridge University Press

Table 1. Stable carbon and oxygen isotope data from the Ordovician succession in the Tingskullen drill core from Öland, southeastern Sweden. Data published in Calner *et al*. (2014) are included in this table.

Drill core depth (m)	Formation	Sample. No.	δ^{13}C	Δ^{18}O	Drill core depth (m)	Formation	Sample No.	δ^{13}C	δ^{18}O
0.1	Persnäs	TK 100	0.49	−6.17	14.5	Skärlöv	TK 71	1.69	−5.57
0.5	Persnäs	TK 99	0.78	−6.05	14.75	Skärlöv	AK 70b	1.69	−5.73
0.75	Persnäs	AK 98b	0.81	−6.23	15.0	Skärlöv	TK 70	1.83	−5.52
1.0	Persnäs	TK 98	0.75	−6.11	15.25	Skärlöv	AK 69b	1.68	−5.66
1.25	Persnäs	AK 97b	0.80	−6.60	15.5	Skärlöv	TK 69	1.95	−5.35
1.5	Persnäs	TK 97	0.91	−5.85					
1.75	Persnäs	AK 96b	0.92	−6.04	15.75	Segerstad	AK 68b	1.78	−5.87
2.0	Persnäs	TK 96	0.75	−6.10	16.0	Segerstad	TK 68	1.84	−5.04
2.25	Persnäs	AK 95b	0.84	−6.18	16.25	Segerstad	AK 67b	1.72	−4.68
2.5	Persnäs	TK 95	0.91	−7.52	16.5	Segerstad	TK 67	1.68	−5.66
2.75	Persnäs	AK 94b	0.88	−6.23	16.75	Segerstad	AK 66b	1.57	−6.06
3.0	Persnäs	TK 94	1.03	−6.29	17.0	Segerstad	TK 66	1.74	−5.23
3.25	Persnäs	AK 93b	0.96	−6.51	17.25	Segerstad	AK 65b	1.71	−5.37
3.5	Persnäs	TK 93	1.02	−6.59	17.5	Segerstad	TK 65	1.56	−4.90
3.75	Persnäs	AK 92b	1.11	−6.48	17.75	Segerstad	AK 64b	1.59	−5.83
4.0	Persnäs	TK 92	0.96	−6.53	18.0	Segerstad	TK 64	1.65	−5.58
4.25	Persnäs	AK 91b	0.88	−7.22	18.25	Segerstad	AK 63b	1.47	−5.84
4.5	Persnäs	TK 91	1.05	−6.09	18.5	Segerstad	TK 63	1.13	−7.76
4.75	Persnäs	AK 90b	1.12	−6.53	18.75	Segerstad	AK 62b	1.49	−6.35
5.0	Persnäs	TK 90	0.96	−5.99	19.0	Segerstad	TK 62	1.23	−5.25
5.25	Persnäs	AK 89b	1.07	−6.89	19.25	Segerstad	AK 61b	1.28	−4.92
5.5	Persnäs	TK 89	1.06	−6.62	19.5	Segerstad	TK 61	1.11	−5.17
5.75	Persnäs	AK 88b	1.06	−6.41	19.75	Segerstad	AK 60b	1.03	−5.86
					20.0	Segerstad	TK 60	1.01	−5.74
6.0	Källa	TK 88	1.09	−6.03	20.1	Segerstad	AK 59e	1.16	−6.19
6.25	Källa	AK 87b	1.10	−6.65	20.2	Segerstad	AK 59d	1.05	−6.27
6.5	Källa	TK 87	1.01	−6.57	20.3	Segerstad	AK 59c	1.06	−5.60
6.75	Källa	AK 86b	0.93	−6.60	20.4	Segerstad	AK 59b	1.03	−5.80
7.0	Källa	TK 86	0.85	−6.44	20.5	Segerstad	TK 59	1.22	−5.31
7.25	Källa	AK 85b	0.98	−6.87	20.6	Segerstad	AK 58e	1.15	−5.90
7.5	Källa	TK 85	1.12	−5.29	20.7	Segerstad	AK 58d	1.14	−5.48
7.75	Källa	AK 84b	1.14	−6.35	20.8	Segerstad	AK 58c	1.19	−5.72
8.0	Källa	TK 84	1.16	−5.84	20.9	Segerstad	AK 58b	1.21	−6.25
8.25	Källa	AK 83b	1.10	−6.08	21.0	Segerstad	TK 58	1.15	−5.75
8.5	Källa	TK 83	1.03	−6.28	21.1	Segerstad	AK 57e	1.29	−5.58
8.75	Källa	AK 82b	1.09	−6.40	21.2	Segerstad	AK 57d	1.29	−6.25
					21.3	Segerstad	AK 57c	1.18	−5.72
9.0	Folkeslunda	TK 82	1.09	−6.33	21.4	Segerstad	AK 57b	1.16	−5.28
9.25	Folkeslunda	AK 81b	1.18	−6.46	21.5	Segerstad	TK 57	1.43	−5.31
9.5	Folkeslunda	TK 81	1.03	−6.92	21.6	Segerstad	AK 56e	1.20	−5.50
9.75	Folkeslunda	AK 80b	1.23	−6.73	21.7	Segerstad	AK 56d	1.30	−5.08
10.0	Folkeslunda	TK 80	0.99	−7.78	21.8	Segerstad	AK 56c	1.32	−4.99
10.25	Folkeslunda	AK 79b	1.34	−6.73	21.9	Segerstad	AK 56b	1.29	−5.66
10.5	Folkeslunda	TK 79	1.30	−6.11					
10.75	Folkeslunda	AK 78b	1.37	−6.58	22.0	Formation C+D	TK 56	1.11	−5.37
11.0	Folkeslunda	TK 78	1.28	−6.12	22.1	Formation C+D	AK 55e	1.17	−5.41
11.25	Folkeslunda	AK 77b	1.49	−5.99	22.2	Formation C+D	AK 55d	1.16	−5.30
11.5	Folkeslunda	TK 77	1.17	−6.14	22.3	Formation C+D	AK 55c	1.05	−5.17
11.75	Folkeslunda	AK 76b	1.55	−6.07	22.4	Formation C+D	AK 55b	0.87	−5.93
					22.5	Formation C+D	TK 55	0.86	−6.54
12.0	Seby	TK 76	1.57	−6.01	22.6	Formation C+D	AK 54e	0.83	−6.23
12.25	Seby	AK 75b	1.63	−5.93	22.7	Formation C+D	AK 54d	0.81	−5.43
					22.8	Formation C+D	AK 54c	0.80	−6.97
12.5	Skärlöv	TK 75	1.64	−5.45	22.9	Formation C+D	AK 54b	0.86	−5.24
12.75	Skärlöv	AK 74b	1.60	−5.89	23.0	Formation C+D	TK 54	0.81	−5.48
13.0	Skärlöv	TK 74	1.60	−4.98	23.1	Formation C+D	AK 53e	0.68	−6.24
13.25	Skärlöv	AK 73b	1.51	−5.55	23.2	Formation C+D	AK 53d	0.72	−6.61
13.5	Skärlöv	TK 73	1.57	−4.77	23.3	Formation C+D	AK 53c	0.69	−6.53
13.75	Skärlöv	AK 72b	1.78	−5.32	23.4	Formation C+D	AK 53b	0.72	−5.46
14.0	Skärlöv	TK 72	1.57	−5.27	23.5	Formation C+D	TK 53	0.67	−6.16
14.25	Skärlöv	AK 71b	1.67	−5.62	23.6	Formation C+D	AK 52e	0.65	−5.59
23.7	Formation C+D	AK 52d	0.76	−5.44	29.6	Gillberga Fm ∗	AK 40e	0.41	−5.75
23.8	Formation C+D	AK 52c	0.74	−5.53	29.7	Gillberga Fm ∗	AK 40d	0.32	−6.68
23.9	Formation C+D	AK 52b	0.68	−5.23	29.8	Gillberga Fm ∗	AK 40c	0.32	−5.98
24.0	Formation C+D	TK 52	0.57	−5.77	29.9	Gillberga Fm ∗	AK 40b	0.34	−6.29
24.1	Formation C+D	AK 51e	0.73	−5.70	30.0	Gillberga Fm ∗	TK 40	0.29	−6.11
24.2	Formation C+D	AK 51d	0.47	−6.56	30.1	Gillberga Fm ∗	AK 39e	0.28	−6.04
24.3	Formation C+D	AK 51c	0.59	−5.50	30.2	Gillberga Fm ∗	AK 39d	0.15	−6.23
24.4	Formation C+D	AK 51b	0.56	−6.45	30.3	Gillberga Fm ∗	AK 39c	0.14	−6.39
24.5	Formation C+D	TK 51	0.62	−5.20	30.4	Gillberga Fm ∗	AK 39b	0.21	−6.30
24.6	Formation C+D	AK 50e	0.47	−6.82	30.5	Gillberga Fm ∗	TK 39	0.29	−5.28
24.7	Formation C+D	AK 50d	0.55	−5.72	30.6	Gillberga Fm ∗	AK 38e	0.22	−6.17

https://doi.org/10.1017/S0016756816000017 Published online by Cambridge University Press

Table 1. Continued

Drill core depth (m)	Formation	Sample. No.	$\delta^{13}C$	$\Delta^{18}O$	Drill core depth (m)	Formation	Sample No.	$\delta^{13}C$	$\delta^{18}O$
24.8	Formation C+D	AK 50c	0.44	−5.49	30.7	Gillberga Fm *	AK 38d	0.32	−5.17
24.9	Formation C+D	AK 50b	0.61	−5.64	30.8	Gillberga Fm *	AK 38c	0.35	−5.93
25.0	Formation C+D	TK 50	0.63	−6.38	30.9	Gillberga Fm *	AK 38b	0.38	−5.89
25.1	Formation C+D	AK 49e	0.69	−5.20	31.0	Gillberga Fm *	TK 38	0.39	−5.62
25.2	Formation C+D	AK 49d	0.59	−5.47	31.1	Gillberga Fm *	AK 37e	0.30	−5.82
25.3	Formation C+D	AK 49c	0.63	−5.71	31.2	Gillberga Fm *	AK 37d	0.08	−6.82
25.4	Formation C+D	AK 49b	0.47	−5.73	31.3	Gillberga Fm *	AK 37c	0.31	−6.28
25.5	Formation C+D	TK 49	0.49	−6.38	31.4	Gillberga Fm *	AK 37b	0.35	−5.59
25.6	Formation C+D	AK 48e	0.56	−5.40	31.5	Gillberga Fm *	TK 37	0.20	−6.63
25.7	Formation C+D	AK 48d	0.46	−6.47	31.6	Gillberga Fm *	AK 36e	0.23	−6.22
25.8	Formation C+D	AK 48c	0.46	−5.60	31.7	Gillberga Fm *	AK 36d	0.34	−5.79
25.9	Formation C+D	AK 48b	0.51	−5.84	31.8	Gillberga Fm *	AK 36c	0.18	−6.68
26.0	Formation C+D	TK 48	0.68	−5.30	31.9	Gillberga Fm *	AK 36b	0.41	−6.23
26.1	Formation C+D	AK 47e	0.53	−5.73	32.0	Gillberga Fm *	TK 36	0.44	−6.10
26.2	Formation C+D	AK 47d	0.45	−6.55	32.1	Gillberga Fm *	AK 35e	0.42	−6.04
26.3	Formation C+D	AK 47c	0.46	−5.96	32.2	Gillberga Fm *	AK 35d	0.40	−5.86
26.4	Formation C+D	AK 47b	0.60	−5.41	32.3	Gillberga Fm *	AK 35c	0.36	−6.67
26.5	Formation C+D	TK 47	0.47	−5.20	32.4	Gillberga Fm *	AK 35b	0.56	−6.01
26.6	Formation C+D	AK 46e	0.55	−6.58	32.5	Gillberga Fm *	TK 35	0.30	−6.39
26.7	Formation C+D	AK 46d	0.47	−5.64	32.6	Gillberga Fm *	AK 34e	0.17	−8.46
26.8	Formation C+D	AK 46c	0.46	−5.98	32.7	Gillberga Fm *	AK 34d	0.53	−6.05
26.9	Formation C+D	AK 46b	0.60	−5.52	32.8	Gillberga Fm *	AK 34c	0.33	−7.16
27.0	Formation C+D	TK 46	0.27	−7.59	32.9	Gillberga Fm *	AK 34b	0.48	−5.70
27.1	Formation C+D	AK 45e	0.47	−5.94	33.0	Gillberga Fm *	TK 34	0.42	−6.23
27.2	Formation C+D	AK 45d	0.29	−6.80	33.1	Gillberga Fm *	AK 33e	0.29	−6.97
27.3	Formation C+D	AK 45c	0.35	−6.20	33.2	Gillberga Fm *	AK 33d	0.19	−6.92
27.4	Formation C+D	AK 45b	0.29	−6.26	33.3	Gillberga Fm *	AK 33c	0.42	−5.87
27.5	Formation C+D	TK 45	0.33	−6.23	33.4	Gillberga Fm *	AK 33b	0.32	−5.96
27.6	Formation C+D	AK 44e	0.42	−6.10	33.5	Gillberga Fm *	TK 33	0.21	−7.25
27.7	Formation C+D	AK 44d	0.30	−6.04	33.6	Gillberga Fm *	AK 32e	0.29	−6.97
27.8	Formation C+D	AK 44c	0.32	−6.46	33.7	Gillberga Fm *	AK 32d	0.45	−6.49
27.9	Formation C+D	AK 44b	0.38	−6.91	33.8	Gillberga Fm *	AK 32c	0.50	−6.31
28.0	Formation C+D	TK 44	0.26	−5.64	33.9	Gillberga Fm *	AK 32b	0.41	−6.79
28.1	Formation C+D	AK 43e	0.31	−5.51	34.0	Gillberga Fm *	TK 32	0.26	−7.08
28.2	Formation C+D	AK 43d	0.39	−6.69	34.1	Gillberga Fm *	AK 31e	0.39	−6.96
28.3	Formation C+D	AK 43c	0.29	−6.28	34.2	Gillberga Fm *	AK 31d	0.40	−6.66
					34.3	Gillberga Fm *	AK 31c	0.44	−5.93
28.4	Gillberga Fm *	AK 43b	0.23	−6.14	34.4	Gillberga Fm *	AK 31b	0.36	−6.27
28.5	Gillberga Fm *	TK 43	0.38	−5.39	34.5	Gillberga Fm *	TK 31	0.27	−6.29
28.6	Gillberga Fm *	AK 42e	0.41	−6.02	34.6	Gillberga Fm *	AK 30e	0.31	−7.54
28.7	Gillberga Fm *	AK 42d	0.44	−7.35	34.7	Gillberga Fm *	AK 30d	0.34	−6.12
28.8	Gillberga Fm *	AK 42c	0.52	−6.05	34.8	Gillberga Fm *	AK 30c	0.27	−6.62
28.9	Gillberga Fm *	AK 42b	0.64	−6.07	34.9	Gillberga Fm *	AK 30b	0.37	−6.34
29.0	Gillberga Fm *	TK 42	0.07	−6.50	35.0	Gillberga Fm *	TK 30	0.37	−6.06
29.1	Gillberga Fm *	AK 41e	0.26	−5.92					
29.2	Gillberga Fm *	AK 41d	0.37	−6.50	35.1	Horns Udde	AK 29e	0.38	−6.08
29.3	Gillberga Fm *	AK 41c	0.34	−6.15	35.2	Horns Udde	AK 29d	0.31	−6.61
29.4	Gillberga Fm *	AK 41b	0.30	−5.20	35.3	Horns Udde	AK 29c	0.24	−7.19
29.5	Gillberga Fm *	TK 41	0.45	−5.26	35.4	Horns Udde	AK 29b	0.30	−5.86
35.5	Horns Udde	TK 29	0.24	−7.10	39.5	Bruddesta	TK 21	0.27	−5.82
35.6	Horns Udde	AK 28e	0.29	−6.54	39.6	Bruddesta	AK 20e	0.25	−6.48
35.7	Horns Udde	AK 28d	0.30	−7.36	39.7	Bruddesta	AK 20d	0.29	−6.21
35.8	Horns Udde	AK 28c	0.38	−7.13	39.8	Bruddesta	AK 20c	0.23	−6.30
35.9	Horns Udde	AK 28b	0.34	−6.15	39.9	Bruddesta	AK 20b	0.46	−6.10
36.0	Horns Udde	TK 28	0.26	−7.59	40.0	Bruddesta	TK 20	0.49	−5.70
36.1	Horns Udde	AK 27e	0.29	−6.91	40.1	Bruddesta	AK 19e	0.37	−6.37
36.2	Horns Udde	AK 27d	0.19	−7.21	40.2	Bruddesta	AK 19d	0.32	−6.18
36.3	Horns Udde	AK 27c	0.40	−6.06	40.3	Bruddesta	AK 19c	0.38	−6.44
36.4	Horns Udde	AK 27b	0.63	−5.85	40.4	Bruddesta	AK 19b	0.45	−6.04
36.5	Horns Udde	TK 27	0.32	−5.92	40.5	Bruddesta	TK 19	0.51	−5.91
36.6	Horns Udde	AK 26e	0.39	−8.19	40.6	Bruddesta	AK 18e	0.58	−6.18
36.7	Horns Udde	AK 26d	0.51	−5.37	40.7	Bruddesta	AK 18d	0.44	−6.07
36.8	Horns Udde	AK 26c	0.57	−5.43	40.8	Bruddesta	AK 18c	0.57	−6.23
36.9	Horns Udde	AK 26b	0.63	−5.61	40.9	Bruddesta	AK 18b	0.24	−7.14
37.0	Horns Udde	TK 26	0.54	−5.45	41.0	Bruddesta	TK 18	0.67	−5.98
37.1	Horns Udde	AK 25e	0.60	−5.42	41.1	Bruddesta	AK 17e	0.48	−6.10
37.2	Horns Udde	AK 25d	0.49	−6.45	41.2	Bruddesta	AK 17d	0.31	−6.12
37.3	Horns Udde	AK 25c	0.53	−5.40	41.3	Bruddesta	AK 17c	0.26	−6.28
37.4	Horns Udde	AK 25b	0.58	−5.53	41.4	Bruddesta	AK 17b	0.53	−6.06
37.5	Horns Udde	TK 25	0.52	−5.79	41.5	Bruddesta	TK 17	0.16	−6.33
37.6	Horns Udde	AK 24e	0.52	−5.71	41.6	Bruddesta	AK 16e	0.33	−6.46
37.7	Horns Udde	AK 24d	0.45	−6.71	41.7	Bruddesta	AK 16d	0.33	−6.24
37.8	Horns Udde	AK 24c	0.62	−5.63	41.8	Bruddesta	AK 16c	0.33	−5.95

Table 1. Continued

Drill core depth (m)	Formation	Sample. No.	$\delta^{13}C$	$\Delta^{18}O$	Drill core depth (m)	Formation	Sample No.	$\delta^{13}C$	$\delta^{18}O$
37.9	Horns Udde	AK 24b	0.69	−5.64	41.9	Bruddesta	AK 16b	0.23	−5.89
					42.0	Bruddesta	TK 16	− 0.04	−6.00
38.0	Bruddesta	TK 24	0.65	−5.65	42.1	Bruddesta	TK 15	0.12	−6.03
38.1	Bruddesta	AK 23e	0.50	−5.93	42.2	Bruddesta	TK 14	0.22	−6.29
38.2	Bruddesta	AK 23d	0.32	−5.93	42.3	Bruddesta	TK 13	0.34	−5.55
38.3	Bruddesta	AK 23c	0.57	−5.45	42.4	Bruddesta	TK 12	0.30	−5.94
38.4	Bruddesta	AK 23b	0.50	−5.56	42.5	Bruddesta	TK 11	0.32	−5.87
38.5	Bruddesta	TK 23	0.45	−5.88	42.6	Bruddesta	TK 10	0.38	−5.81
38.6	Bruddesta	AK 22e	0.62	−5.70	42.7	Bruddesta	TK 9	0.18	−6.00
38.7	Bruddesta	AK 22d	0.38	−5.96					
38.8	Bruddesta	AK 22c	0.45	−5.73	42.9	Köpingsklint	TK 7	0.04	−6.16
38.9	Bruddesta	AK 22b	0.31	−5.88	43.0	Köpingsklint	TK 6	0.06	−6.09
39.0	Bruddesta	TK 22	0.35	−5.82	43.1	Köpingsklint	TK 5	0.24	−5.62
39.1	Bruddesta	AK 21e	0.13	−6.33	43.2	Köpingsklint	TK 4	0.46	−6.02
39.2	Bruddesta	AK 21d	0.47	−5.71	43.3	Köpingsklint	TK 3	0.81	−6.10
39.3	Bruddesta	AK 21c	0.44	−6.13	43.4	Köpingsklint	TK 2	0.63	−6.23
39.4	Bruddesta	AK 21b	0.37	−5.81					

Gillberga Fm ∗ – Gillberga Fm (Formation A + B)

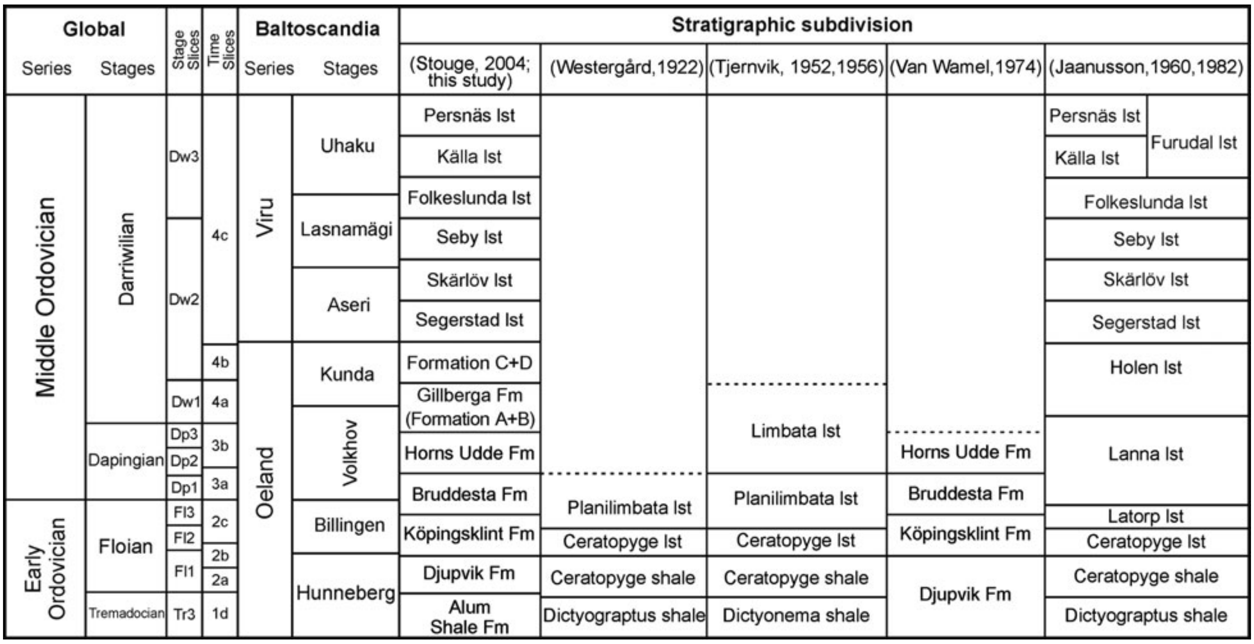

Figure 2. Stratigraphic subdivision and unit names previously proposed for the Ordovician in Öland. lst – limestone.

provided an overview on the stratigraphic terminology for the sedimentary succession on Öland, which is followed herein (Fig. 2). The Tingskullen core records the entire Lower and Middle Ordovician succession that is preserved on the island, including in ascending order the Djupvik, Köpingsklint, Bruddesta and Horns Udde formations, the Gillberga Formation (Formation A + B), Formation C + D, and the Segerstad, Skärlöv, Seby, Folkeslunda, Källa and Persnäs limestones (Fig. 3). All these formations are dominated by a fine-grained limestone with a bioclast composition typical for cool-water carbonates, i.e. devoid of reef-building biota or precipitated carbonate grains such as ooids. Calner *et al.* (2014) included a description of the lithological succession of this core and we only briefly outline the lithofacies for each formation herein.

The Djupvik Formation is composed of brownish shale with a thickness of 2 m, while the overlying Köpingsklint Formation is 0.5 m thick and dominated by grey, slightly pink lime mudstone and wackestone rich in trilobite and brachiopod bioclasts and a few glauconitic beds (Fig. 4a). The Bruddesta Formation consists of grey, reddish wackestone to packstone with many discontinuity surfaces and hardgrounds (Fig. 4b). Here, the most remarkable bed is the colourful 'Blommiga Bladet' hardground complex, which is widespread in Baltoscandia. The 2.5 m thick Horns Udde Formation is characterized by pale red to grey wackestone and packstone (Fig. 4c), which is overlain by the 6.7 m thick Gillberga Formation (Formation A + B) mainly composed of wackestone with abundant glauconite (Fig. 4d). Formation C + D (6.3 m) is dominated by grey packstone and grainstone with some

https://doi.org/10.1017/S0016756816000017 Published online by Cambridge University Press

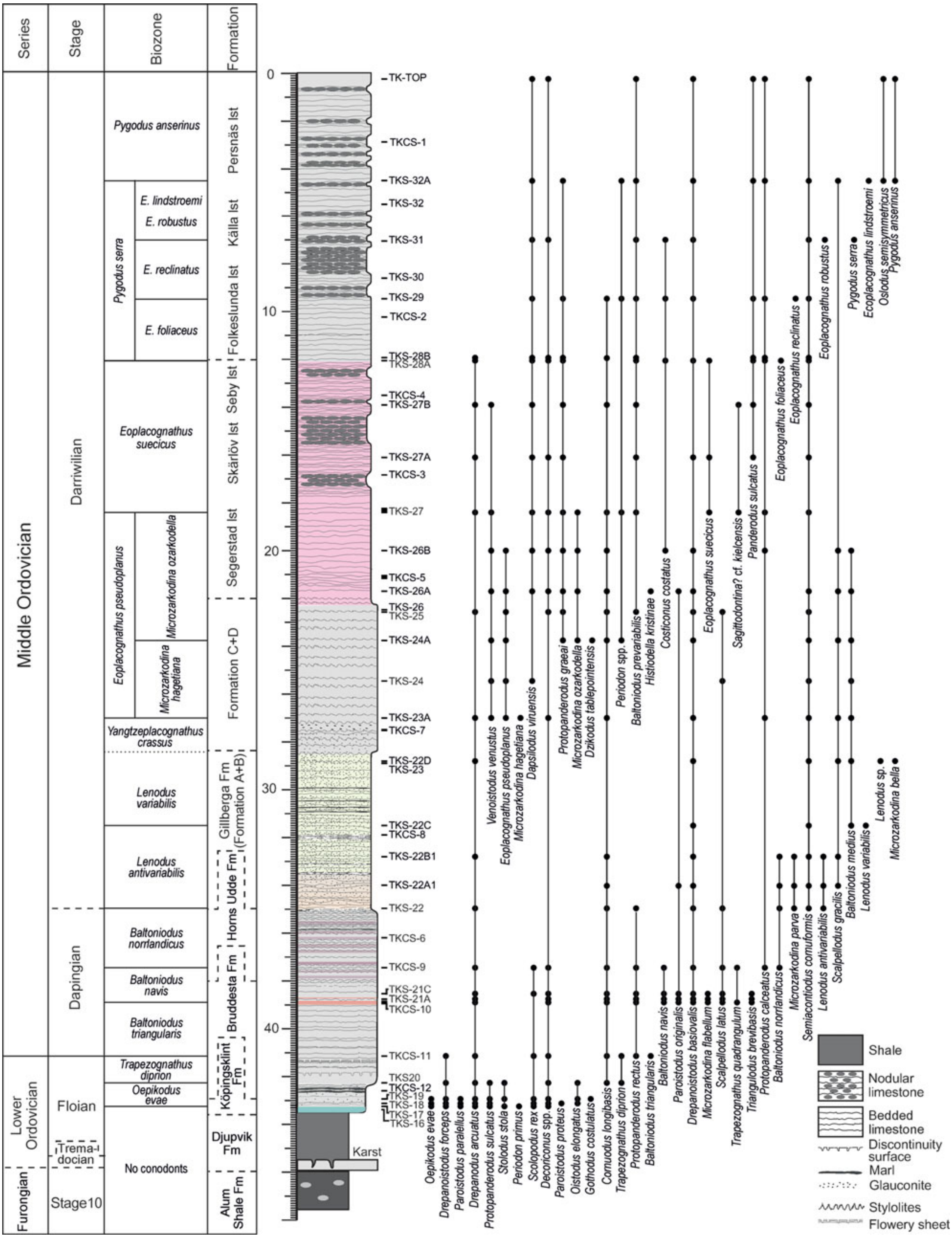

Figure 3. Stratigraphy, distribution of conodont taxa and biostratigraphic subdivision of the Ordovician succession in the Tingskullen drill core from Öland.

coarser glauconite distributed in the lower part of the formation (Fig. 4e). The Segerstad Limestone is ~6.3 m thick and mainly comprises reddish wackestone and packstone (Figs 4f, 5a), while the overlying 3.3 m thick succession with red nodular wackestone and subordinate mudstone and packstone is referred to as the Skärlöv Limestone (Fig. 5b, c). The Seby Limestone is ~0.4 m thick and characterized by variegated, pale reddish wackestone. The Folkeslunda Limestone is composed of grey packstone with a thickness of 2.9 m

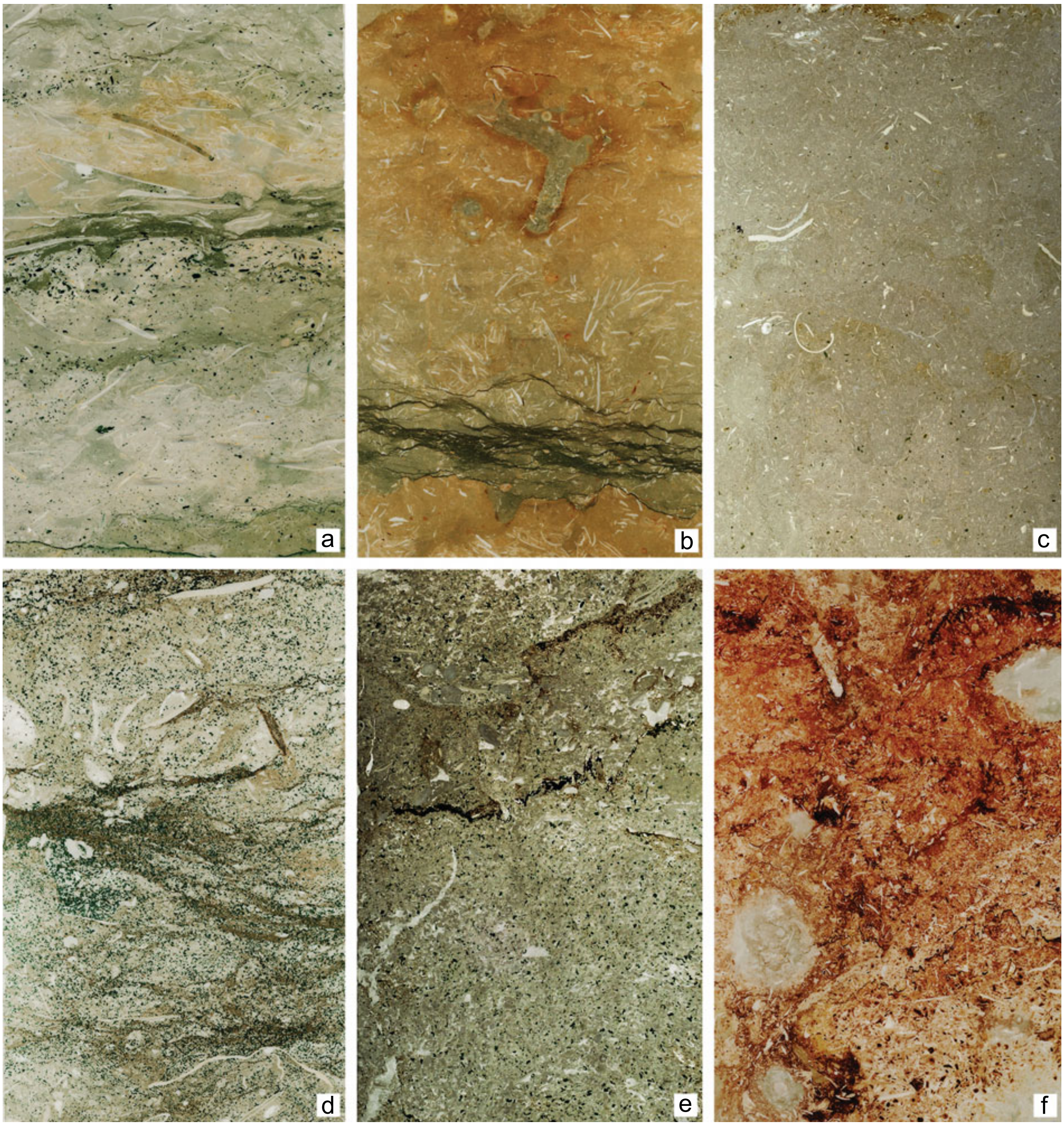

Figure 4. Photoplate showing typical microfacies of the Tingskullen drill core. The width of each photograph is 40 mm, corresponding to the diameter of the core. (a) Skeletal wackestone with abundant glauconite grains in the Köpingsklint Formation (TKS-18). (b) Skeletal wackestone with thin clay seams, a hardground surface and borings. Note abundant, delicate bioclasts from trilobites (TKCS-11); lower part of the Bruddesta Formation. (c) Mudstone–wackestone with bioturbation (TKCS-9); lower part of the Horns Udde Formation. (d) Wackestone with abundant glauconite (TKCS-8); middle part of the Gillberga Formation (Formation A + B). (e) Packstone–grainstone with abundant glauconite (TKCS-7); lower part of Formation C + D. (f) Reddish grainstone of the lower Segerstad Limestone (TKCS-5).

(Fig. 5d). The Källa Limestone is ~3.1 m thick and comprises grey wackestone and packstone interbedded with finely nodular limestone (Fig. 5e). The topmost unit in the core and on the island is the Persnäs Limestone (~5.9 m in the core). It is characterized by grey wackestone with interbeds of finely nodular limestone. (Fig. 5f)

3. Material and methods

The Tingskullen core was recovered in 2010 from the northeastern part of the island of Öland (about 700 m NE of the church ruin at Källa Hamn, and south of Tingskullsgatan at N 57.116172, E 16.993013; Fig. 1). The total length of the core is 111 m (Ø 40 mm) and drilling was terminated a few metres down in quartz arenites of the Cambrian Series 2. The Ordovician part of the core is ~46 m thick. The core is stored at the Department of Geology, Lund University.

A total of 29 conodont samples were collected from the core in order to constrain the carbon isotope chemostratigraphy. The conodont samples were processed at the Department of Geology, Lund University, with

https://doi.org/10.1017/S0016756816000017 Published online by Cambridge University Press

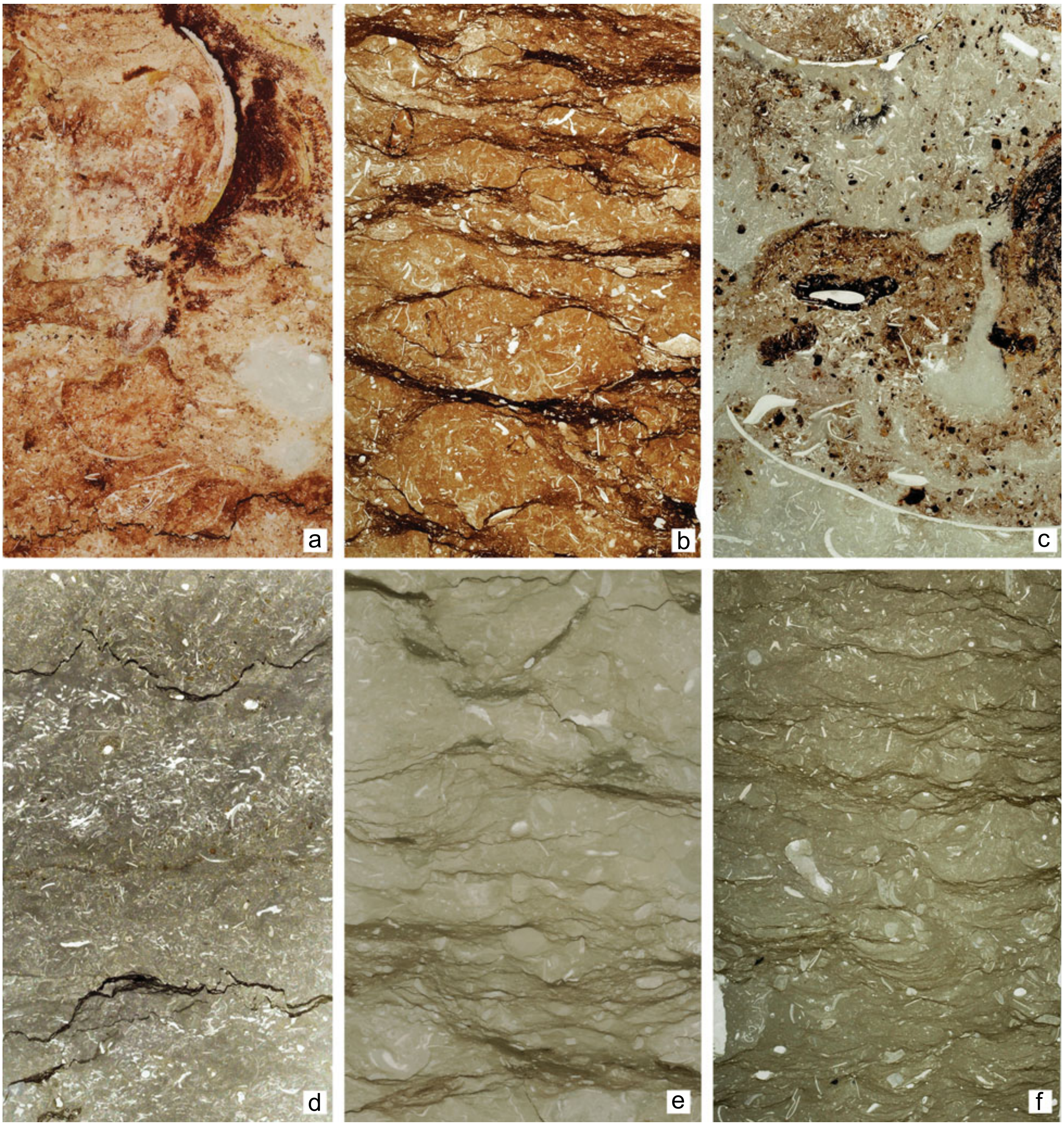

Figure 5. Photoplate showing typical microfacies of the Tingskullen drill core. The width of each photograph is 40 mm, corresponding to the diameter of the core. (a) Reddish packstone–grainstone from the upper Segerstad Limestone (TKS-27). (b) Argillaceous, reddish wackestone with thin, irregular clay seams (TKCS-3); lower part of the Skärlöv Limestone. (c) Bioturbated skeletal packstone with borings (TKCS-4); upper part of the Skärlöv Limestone. (d) Bioturbated wackestone of the Folkeslunda Limestone (TKCS-2). (e) Argillaceous, bioturbated and nodular mudstone–wackestone with thin clay partings in the Källa Limestone (TKS-30). (f) Argillaceous, nodular wackestone–packstone with thin clay partings in the Persnäs Limestone (TKCS-1).

diluted, buffered acetic acid, and the residues were separated by use of heavy liquid (sodium polytungstate) following the techniques proposed by Jeppsson, Anehus & Fredholm (1999). All residues were hand-picked for conodonts, and all conodont elements were well preserved exhibiting a Colour Alteration Index (CAI) of 1 (cf. Epstein, Epstein & Harris, 1977). The photographs of the figured specimens were taken in a Scanning Electron Microscope (Hitachi 3400N). All figured elements (LO12096t through LO12162t; repository number LO – for Lund Original) are stored in the type collection at the Department of Geology, Lund University.

For $\delta^{13}C_{carb}$ analysis, sample powders were recovered from the fresh core surface by use of a handheld electric drill with a drill bit that had a diameter of ~1–2 mm. Samples were recovered from the matrix of the rock while larger bioclasts and calcite veins were avoided.

Carbonate powders were reacted with 100 % phosphoric acid at 70 °C using a Gasbench II connected to a ThermoFinnigan Five Plus mass spectrometer. The analyses were carried out at the Geocentre of Northern Bavaria in Erlangen (Germany), and all values are reported in per mil relative to the V-PDB (Vienna Pee Dee Belemnite) by assigning $\delta^{13}C$ and $\delta^{18}O$ values +1.95 ‰ and −2.20 ‰ to international standard NBS19 and −46.6 ‰ and −26.7 ‰ to international standard LSVEC, respectively. Uncertainties of better than ± 0.05 ‰ (1σ) for $\delta^{13}C$ and better than ± 0.07 ‰ (1σ) for $\delta^{18}O$ analyses were checked by replicate analyses of laboratory standards calibrated to NBS19 and LSVEC.

4. Results

4.a. Conodont biostratigraphy

In the Ordovician limestone succession of the Tingskullen core, more than 50 conodont species belonging to 29 genera have been identified, and 12 conodont zones and 6 subzones have been recognized. These are the *Oepikodus evae*, *Trapezognathus diprion*, *Baltoniodus triangularis*, *B. navis*, *B. norrlandicus*, *Lenodus antivariabilis*, *L. variabilis*, *Yangtzeplacognathus crassus*, *Eoplacognathus pseudoplanus*, *E. suecicus*, *Pygodus serra* and *P. anserinus* zones in ascending order. In addition, the *E. pseudoplanus* Zone is subdivided into two subzones, i.e. the *Microzarkodina hagetiana* Subzone and the overlying *M. ozarkodella* Subzone, while the *P. serra* Zone comprises the *E. foliaceus*, *E. reclinatus*, *E. robustus* and *E. lindstroemi* subzones in ascending order (Fig. 3).

4.a.1. Oepikodus evae *Zone (c. 42.27–43.24 m)*

Lindström (1971) introduced the *O. evae* Zone in the Baltoscandian succession. In the present study, the definition of the *Oepikodus evae* Zone agrees with that of Bagnoli & Stouge (1997), characterized at the base by the first appearance (FAD) of the index species and at the top by the FAD of *Trapezognathus diprion* (Fig. 6u). The *O. evae* Zone in the Tingskullen core can be correlated to the lower part of the *O. evae* Zone of Lindström (1971), where *O. evae* (Fig. 7q, r) is abundant. Besides *O. evae*, *Drepanoistodus forceps* (Fig. 7s, t), *Paroistodus proteus*, *Oistodus lanceolatus* (Fig. 7x, y) and *Stolodus stola* are quite common in this zone. In addition, *Periodon flabellum* (Fig. 7aa), *Protopanderodus rectus* (Fig. 7ad, ae) and *Paroistodus parallelus* (Fig. 7ab, ac) are present. The *O. evae* Zone has been reported from South China, Argentina and North America (Serpagli, 1974; An, 1987; Stouge & Bagnoli, 1988). This zone is middle Floian in age.

4.a.2. Trapezognathus diprion *Zone (c. 41.14–42.27 m)*

Bagnoli & Stouge (1997) defined this zone as representing the interval ranging from the FAD of *Trapezognathus diprion* to the FAD of *Microzarkodina russica* according to the succession on Öland, Sweden. However, *Microzarkodina russica* is absent in our material from the Tingskullen core, which may be owing to the small number of core samples. The top of the present *T. diprion* Zone, however, is marked by the base of the overlying *Baltoniodus triangularis* Zone. The associated fauna includes *D. forceps*, *Oistodus lanceolatus*, *Stolodus stola*, *Cornuodus longibasis*, etc. *O. evae* disappears in this zone. This zone in the present study is interpreted to be late Floian in age, coinciding with the upper *O. evae* Zone of Lindström (1971), and including the *T. diprion* and *M. russica* zones of Bagnoli & Stouge (1997). The same zone was also reported from South China (Li *et al*. 2010).

4.a.3. Baltoniodus triangularis *Zone (c. 38.9–41.14 m)*

This zone starts with the FAD of *Baltoniodus triangularis*, while its top is marked by the FAD of *B. navis*. Only one sample (TKCS-11) yielding the index taxon (Fig. 7a–e) was recovered from the Tingskullen core. Other species in this level are represented by *Protopanderodus rectus*, *T. diprion*, *Scolopodus rex*, *D. forceps* and *C. longibasis*. *B. triangularis*, which has a wide palaeogeographic distribution, has been ratified as the index species of the basal Dapingian (Wang *et al*. 2005, 2009). Thus, the *B. triangularis* Zone in this study could be correlated to the *B. triangularis* and *Microzarkodina flabellum* zones of Bagnoli & Stouge (1997), and indicates an early Dapingian age.

4.a.4. Baltoniodus navis *Zone (c. 37.45–38.9 m)*

The base of the *B. navis* Zone is marked by the FAD of *B. navis* (Fig. 7f–h), and its top by the FAD of *B. norrlandicus*. Except for *B. navis*, five other important species, i.e. *Paroistodus originalis* (Fig. 7v, w), *Drepanoistodus basiovalis* (Fig. 7u), *M. flabellum* (Fig. 6r), *Scalpellodus latus* and *Trapezognathus quadrangulum*, occur in this zone in the Tingskullen core for the first time. An abundance of *P. originalis* may indicate that the present interval of the *B. navis* Zone can be correlated to the *P. originalis* Zone of Löfgren (1994).

4.a.5. Baltoniodus norrlandicus *Zone (c. 34.95–37.45 m)*

Bagnoli & Stouge (1997) introduced this zone for the Ordovician succession on Öland, characterized at the base by the FAD of *B. norrlandicus* (Fig. 7i, j). Its top is defined by the FAD of *Lenodus antivariabilis*. This zone is recorded in the Horns Udde Formation. *Protopanderodus calceatus* appears in this zone, and other associated species including *P. rectus*, *D. basiovalis*, *Microzarkodina parva* (Fig. 6p, q) and *S. latus* are common. A similar faunal assemblage, i.e. the *B. norrlandicus–M. parva* Zone, was observed on the Yangtze Platform succession by Wang & Bergström (1999). They argued that the base of the Darriwilian is located in the upper part of this zone.

https://doi.org/10.1017/S0016756816000017 Published online by Cambridge University Press

Figure 6. Conodonts from the Tingskullen drill core. (a, b) *Eoplacognathus reclinatus* (Fåhræus): (a) Pa element from sample TKS-29, LO12096t; (b) Pb element from sample TKS-29, LO12097t. (c, d) *Eoplacognathus robustus* (Bergström), Pb elements from sample TKS-31, LO12098t, LO12099t. (e, f) *Eoplacognathus lindstroemi* (Hamar): (e) Pb element from sample TKS-32A, LO12100t; (f) Pa element from sample TKS-32A, LO12101t. (g) *Histiodella kristinae* Stouge, P element from sample TKS-26A, LO12102t. (h–j) *Eoplacognathus pseudoplanus* (Viira): (h) M element from sample TKS-23A, LO12103t; (i) Pb element from sample TKS-23A, LO12104t; (j) Pa element from sample TKS-23A, LO12105t. (k, l) *Lenodus antivariabilis* (An): (k) Sb element from sample TKS-22A1, LO12106t; (l) M element from sample TKS-22B1, LO12107t. (m–o) *Lenodus variabilis* (Sergeeva): (m) Pa element from sample TKS-22C, LO12108t; (n) Sc element from sample TKS-22C, LO12109t; (o) Pb element from sample TKS-22C, LO12110t. (p, q) *Microzarkodina parva* Lindström: (p) P element from sample TKS-22A1, LO12111t; (q) P element from sample TKCS-9, LO12112t. (r) *Microzarkodina flabellum* (Lindström), P element from sample TKCS-10, LO12113t. (s) *Microzarkodina hagetiana* Stouge & Bagnoli, P element from sample TKS-23A, LO12114t. (t) *Microzarkodina ozarkodella* Lindström, P element from sample TKS-24A, LO12115t. (u) *Trapezognathus diprion* (Lindström), P element from sample TKS-20, LO12116t. (v) *Eoplacognathus foliaceus* (Fåhræus), Pb element from sample TKS-28A, LO12117t. (w) *Sagittodontina*? cf. *kielcensis* (Dzik), Pb element from sample TKS-27B, LO12118t. (x, y) *Lenodus* sp.: (x) Pb element from sample TKS-22D, LO12119t; (y) Sc element from sample TKS-22D, LO12120t. (z) *Pygodus serra* (Hadding), Pa element from sample TKS-31, LO12121t. (aa) *Pygodus anserinus* Lamont & Lindström, Pa element from sample TKS-32A, LO12122t. (ab, ac) *Oslodus semisymmetricus* (Hamar): (ab) M element from sample TK-TOP, LO12123t; (ac) S element from sample TK-TOP, LO12124t. (ad) *Panderodus sulcatus* (Fåhræus), S element from sample TK-TOP, LO12125t. (ae) *Venoistodus venustus* (Stauffer), M element from sample TKS-27, LO12126t. (af) *Costiconus costatus* (Dzik), S element from sample TKS-27, LO12127t. (ag, ah) *Protopanderodus calceatus* Bagnoli & Stouge: (ag) S element from sample TKS-27, LO12128t; (ah) M element from sample TKS-27, LO12129t.

4.a.6. Lenodus antivariabilis *Zone (c. 31.5–34.95 m)*

The *Lenodus antivariabilis* Zone was established by An (1981) based on the material from the Yangtze Platform. This zone can also be traced to Baltoscandia (Zhang, 1998*b*). The *L. antivariabilis* Zone was defined by the FAD of the index species (Fig. 6k, l). Bagnoli & Stouge (1997) reported this zone from Öland. In the Tingskullen core, a few elements of *L. antivariabilis* are found in three samples (TKS-22, TKS-22A1,

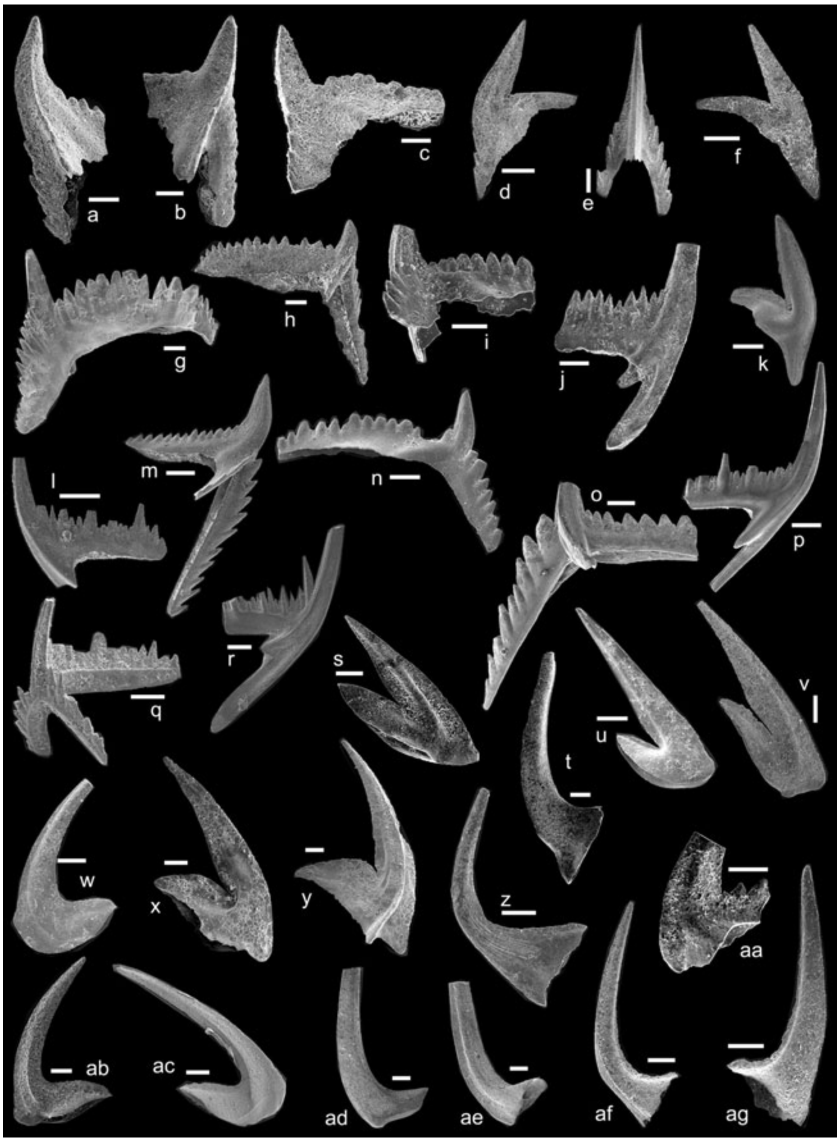

Figure 7. Conodonts from the Tingskullen drillcore. (a–e) *Baltoniodus triangularis* (Lindström): (a) Pb element from sample TKCS-11, LO12130t; (b) Pa element from sample TKCS-11, LO12131t; (c) Pa element from sample TKCS-11, LO12132t; (d) M element from sample TKCS-11, LO12133t; (e) Sa element from sample TKCS-11, LO12134t. (f–h) *Baltoniodus navis* (Lindström): (f) M element from sample TKS-21C, LO12135t; (g) Pa element from sample TKCS-10, LO12136t; (h) Pa element from sample TKS-21A, LO12137t. (i, j) *Baltoniodus norrlandicus* (Löfgren): (i) Pb element from sample TKCS-9, LO12138t; (j) Sc element from sample TKCS-9, LO12139t. (k–n) *Baltoniodus prevariabilis* (Fåhræus): (k) M element from sample TK-TOP, LO12140t; (l) Sc element from sample TK-TOP, LO12141t; (m) Pb element from sample TK-TOP, LO12142t; (n) Pa element from sample TK-TOP, LO12143t. (o, p) *Baltoniodus medius* (Dzik): (o) Pa element from sample TKS-24A, LO12144t; (p) Sc element from sample TKS-24A, LO12145t. (q, r) *Oepikodus evae* (Lindström): (q) P element from sample TKS-16, LO12146t; (r) S element from sample TKS-17, LO12147t. (s, t) *Drepanoistodus forceps* (Lindström): (s) M element from sample TKS-17, LO12148t; (t) S element from sample TKS-17, LO12149t. (u) *Drepanoistodus basiovalis* (Sergeeva), M element from sample TKCS-10, LO12150t. (v, w) *Paroistodus originalis* (Sergeeva): (v) M element from sample TKCS-10, LO12151t; (w) S element from sample TKCS-10, LO12152t. (x, y) *Oistodus lanceolatus* Pander: (x) M element from sample TKS-18, LO12153t; (y) Sb element from sample TKS-19, LO12154t. (z) *Dapsilodus viruensis* (Fåhræus), S element from sample TKS-26B, LO12155t. (aa) *Periodon flabellum* (Lindström), Pa element from sample TKS-17, LO12156t. (ab, ac) *Paroistodus parallelus* (Pander), S elements from sample TKS-18, LO12157t, LO12158t. (ad, ae) *Protopanderodus rectus* (Lindström): (ad) S element from sample TKCS-11, LO12159t; (ae) M element from sample TKCS-11, LO12160t. (af, ag) *Triangulodus brevibasis* (Sergeeva): (af) Sb element from sample TKS-21A, LO12161t; (ag) P element from sample TKS-21A, LO12162t.

TKS-22B1) from the lower part of the Gillberga Formation (Formation A + B). The conodont fauna is dominated by advanced elements of *B. norrlandicus*, *D. basiovalis* and *Semiacontiodus cornuformis*. Other important taxa, i.e. *M. parva* (Fig. 6p, q), *Triangulodus brevibasis* (Fig. 7af, ag) and *Scalpellodus gracilis*, appear in this zone, but are not frequent in this interval. This zone was interpreted to be earliest Darriwilian in age (Zhang, 1998*b*; Wang & Bergström, 1999).

4.a.7. Lenodus variabilis *Zone (c. 28.8–31.5 m)*

Lenodus variabilis is present in sample TKS-22C (Fig. 6m–o) from the middle part of the Gillberga

https://doi.org/10.1017/S0016756816000017 Published online by Cambridge University Press

Formation (Formation A + B). The *L. variabilis* Zone is marked at the base by the FAD of the nominate species, and its top is characterized by the FAD of *Y. crassus*. This zone has been widely reported from the Baltoscandian and Yangtze platforms (Zhang, 1998*a*,*b*; Löfgren, 2003). Only one sample from the upper part of the Gillberga Formation (Formation A + B) yields a few elements of *L. variabilis*, indicating the presence of the *L. variabilis* Zone. Besides the index taxon, the conodont fauna includes *Baltoniodus medius*, *S. cornuformis* and *D. basiovalis*. Zhang (1998*b*) documented that *B. medius* occurred in the upper *L. variabilis* Zone on the Yangtze Platform for the first time. Thus, it may indicate that the interval of the *L. variabilis* Zone present in the Tingskullen core only represents the upper part of the zone.

4.a.8. Yangtzeplacognathus crassus *Zone (c. 27.0–28.8 m)*

Zhang (1998*b*) introduced the *Y. crassus* Zone based on the Middle Ordovician succession on the Yangtze Platform. The *Y. crassus* Zone is characterized by the FAD of the nominate species. The *Y. crassus* Zone has been reported by Löfgren (2000) in the uppermost Gillberga Formation from the Gillberga quarry, northern Öland. In the Tingskullen core, however, we have not found *Y. crassus*, which may be owing to the small sampling size herein. However, a few advanced elements of *Lenodus* (*Lenodus* sp., Fig. 6x, y) occurred in sample TKS-22D. Thus, we provisionally locate the *Y. crassus* Zone just above the level of TKS-22D with a thickness of 1.8 m in the uppermost Gillberga Formation (Formation A + B). The conodont fauna is dominated by *B. medius*. Other species present include *Microzarkodina bella*, *S. gracilis*, *D. basiovalis* and *Drepanodus arcuatus*.

4.a.9. Eoplacognathus pseudoplanus *Zone:* Microzarkodina hagetiana *Subzone (c. 23.75–27.0 m)*

The *E. pseudoplanus* Zone was introduced by Viira (1974) for the upper Kunda Stage. It can be subdivided into two subzones, i.e. the *M. hagetiana* and *M. ozarkodella* subzones in ascending order (Zhang, 1998*a*). According to the material from the Yangtze Platform, Zhang (1998*b*) correlated the *E. pseudoplanus* Zone with the *Dzikodus tablepointensis* Zone. The *M. hagetiana* Subzone is marked by the disappearance of *Y. crassus* (Zhang, 1998*b*). This subzone yields *E. pseudoplanus* (Fig. 6h–j) and is represented by two samples (TKS-23A, TKS-24) in the Tingskullen core and has a thickness of approximately 3.25 m. *B. medius* and *S. cornuformis* are common. Other associated species are *M. hagetiana* (Fig. 6s), *D. arcuatus*, *C. longibasis*, *D. basiovalis*, *S. latus*, *S. gracilis*, *Venoistodus venustus* and *Dapsilodus viruensis*.

4.a.10. Eoplacognathus pseudoplanus *Zone:* Microzarkodina ozarkodella *Subzone (c. 18.4–23.75 m)*

The base of this subzone is defined by the FAD of *M. ozarkodella* (Fig. 6t). The characteristic *M. ozarkodella* was recovered in sample TKS-24A. This subzone has a thickness of 5.35 m, ranging from 18.4 m to 23.75 m in the Tingskullen core. *B. medius*, *D. basiovalis* and *D. viruensis* are quite common in this subzone. Other taxa appearing in this subzone for the first time include *Protopanderodus graeai*, *Dzikodus tablepointensis*, *Baltoniodus prevariabilis* (Fig. 7k–n), *Histiodella kristinae* (Fig. 6g) and *Costiconus costatus*. *Dapsilodus viruensis* (Fig. 7z) is present in this subzone and ranges up to the top of the core section.

4.a.11. Eoplacognathus suecicus *Zone (c. 12.05–18.4 m)*

Bergström (1971) established the *E. suecicus* Subzone within the *Pygodus serra* Zone. However, the following studies proposed a separate *E. suecicus* Zone, marked by the FAD of the nominate species (Löfgren, 1978; Zhang & Sturkell, 1998). This definition is followed herein. The *E. suecicus* Zone is about 6.35 m thick in the Tingskullen core, including the upper Segerstad, Skärlöv and Seby limestones. Apart from *E. suecicus*, *Sagittodontina*? cf. *kielcensis* (Fig. 6w) and *Panderodus sulcatus* (Fig. 6ad) occur in this zone for the first time. Other taxa, such as *B. prevariabilis*, *P. graeai*, *D. viruensis* and *S. cornuformis*, are very common and associated with *C. costatus* (Fig. 6af), *V. venustus* (Fig. 6ae) and *P. calceatus* (Fig. 6ag, ah).

4.a.12. Pygodus serra *Zone:* Eoplacognathus foliaceus *Subzone (c. 9.45–12.05 m)*

We follow the definition of the *E. foliaceus* Subzone by Bergström (1971). Its base is marked by the FAD of the nominate species (Fig. 6v), while its top is characterized by the FAD of *E. reclinatus*. A few specimens of *E. foliaceus* occur in sample TKS-28A. Besides *E. foliaceus*, *P. graeai*, *D. basiovalis*, *S. cornuformis*, *B. prevariabilis*, *D. viruensis* and *P. sulcatus* are common in this interval. Most of the taxa extend into the following zone. *P. serra* is absent in this subzone.

4.a.13. Pygodus serra *Zone:* Eoplacognathus reclinatus *Subzone (c. 7.0–9.45 m)*

The *E. reclinatus* Subzone is marked by the FAD of the index species (Fig. 6a, b). In the Tingskullen core, the *E. reclinatus* Subzone has a thickness of 2.45 m. The conodont fauna is dominated by *B. prevariabilis*, *P. graeai* and *D. viruensis*. The *E. reclinatus* Subzone is quite common in Baltoscandia.

4.a.14. Pygodus serra *Zone:* Eoplacognathus robustus *and* E. lindstroemi *subzones (c. 4.5–7.0 m)*

As demonstrated by Bergström (1971), the base of the *E. robustus* Subzone is characterized by the FAD of the nominate species (Fig. 6c, d). In the Tingskullen core, this subzone is 2.5 m thick. Apart from *E. robustus*, *P. serra* (Fig. 6z) occurs in this subzone in the Tingskullen core for the first time. Other commonly associated species include *B. prevariabilis*, *C. costatus*, *D. viruensis*, *S. cornuformis* and *D. basiovalis*.

The overlying *E. lindstroemi* Subzone is not recorded from the Tingskullen core, which presumably is caused by too widely spaced samples. But the index species of the *E. lindstroemi* Subzone of the *P. serra* Zone has been recovered only from the base of the overlying *P. anserinus* Zone where *E. lindstroemi* co-occurs with *P. anserinus* in sample TKS-32A.

4.a.15. Pygodus anserinus *Zone (c. 0–4.5 m)*

The topmost 4.5 m in the Tingskullen core are correlated to the *P. anserinus* Zone. This zone was introduced by the FAD of *P. anserinus* (Fig. 6aa). Most of the species that occurred in this zone are extended from the underlying *P. serra* Zone. *P. sulcatus*, *B. prevariabilis*, *D. basiovalis* and *S. cornuformis* are quite common in this part of the succession. Except for the index species, *Oslodus semisymmetricus* (Fig. 6ab, ac) and *E. lindstroemi* (Fig. 6e, f) are recorded at the base of this zone for the first time (sample TKS-32A).

4.b. $\delta^{13}C_{carb}$ chemostratigraphy

The carbon isotope stratigraphy of the Tingskullen core was first dealt with by Calner *et al*. (2014). Their dataset is herein expanded and related to the conodont biostratigraphy presented above (Fig. 8).

A low variability in the $\delta^{13}C_{carb}$ dataset can be seen in the interval spanning the Köpingsklint Formation to the Gillberga Formation (Formation A + B). There, the values vary between *c*. 0 and 0.8 ‰. A prominent positive trend is detected in the Bruddesta Formation in which $\delta^{13}C_{carb}$ values increase from *c*. 0.05 ‰ to *c*. 0.6 ‰ in the *O. evae* and *B. triangularis* zones. Another positive trend is present from the upper Bruddesta Formation to the lower Horns Udde Formation, corresponding to the upper *B. triangularis* through the lower *B. norrlandicus* zones. A minor negative shift in $\delta^{13}C_{carb}$ values is observed in the upper Horns Udde Formation, biostratigraphically corresponding to the upper *B. norrlandicus* Zone. Low values, scattering between 0.2 ‰ and 0.5 ‰, are recorded from an interval spanning the *L. antivariabilis* and *Y. crassus* zones in the Gillberga Formation (Formation A + B).

The complete MDICE with a clear rising limb, peak interval and falling limb is observed through the middle and upper parts of the Tingskullen core. $\delta^{13}C_{carb}$ values of the MDICE start to increase within the *M. hagetiana* Subzone in the middle part of Formation C + D, and reach a first peak with values of about 1.2 ‰ in the lowermost Segerstad Limestone (middle *M. ozarkodella* Subzone). This first peak is followed by a minor negative shift in the upper *M. ozarkodella* Subzone. Thus, the rising limb of the MDICE largely covers the *E. pseudoplanus* Zone. The major positive shift of the MDICE, reaching between *c*. 1.5 and 2.0 ‰ (peak value at 1.95 ‰), occurs in the *E. suecicus* Zone. The peak interval of the MDICE spans the upper Segerstad, Skärlöv and Seby limestones. The falling limb of the MDICE starts in the *E. foliaceus* Subzone of the *P. serra* Zone, while lower $\delta^{13}C_{carb}$ values scattered around the baseline values of about 1 ‰ are recognized in the interval correlated to the *E. reclinatus* and *E. robustus* subzones of the *P. serra* Zone just before a continuous negative trend in the $\delta^{13}C_{carb}$ values is documented from the *P. anserinus* Zone in the topmost part of the Tingskullen core.

5. Discussion

5.a. Diagenesis in the Tingskullen succession

Our petrographic observations demonstrate that the analysed samples include lime mudstone, wackestone and some packstone, with bioclasts dominated by trilobites, brachiopods, cephalopods and echinoderms. Conodont elements from the Tingskullen core display CAI values of 1, suggesting that the Ordovician succession in this core is thermally nearly unaltered. The cross-plot of $\delta^{13}C_{carb}$ and $\delta^{18}O_{carb}$ shows no obvious correlation between them ($R^2 = 0.1136$), and the values of $\delta^{18}O_{carb}$ are from 4.5 ‰ to 8.5 ‰ (Fig. 9), indicating that the samples from the Tingskullen core have great potential to preserve primary carbon isotope signatures (cf. Banner & Hanson, 1990; Marshall, 1992).

5.b. Potential for correlation of the $\delta^{13}C_{carb}$ record

In this section we evaluate the potential for correlation of the Tingskullen core $\delta^{13}C_{carb}$ record. Ainsaar *et al*. (2010) documented a composite carbon isotope curve for the Middle and Upper Ordovician of Baltoscandia based on data from drill cores and outcrop sections in Estonia, Latvia and Sweden. They subdivided their $\delta^{13}C_{carb}$ composite profile into 17 carbon isotopic zones, referred to as Baltic Carbon (BC) 1–17, of which BC1 marked the base of the Dapingian. With the exception of those from the Köpingsklint and lower Bruddesta formations, the data from the Ordovician succession in the Tingskullen core are largely assigned to the lowermost four isotopic zones of Ainsaar *et al*. (2010), i.e. BC1–BC4. The BC1 zone includes the lower part of the Tingskullen core with low values of $\delta^{13}C_{carb}$ spanning the upper Bruddesta Formation through Gillberga Formation, an interval that comprises the *B. triangularis* to *Y. crassus* conodont zones. Although there is only little variation in the $\delta^{13}C_{carb}$ values in the lower part of the Tingskullen core, it merits making a detailed intra- and intercontinental correlation when supported by conodont biostratigraphy. A positive shift in $\delta^{13}C_{carb}$ values occurs during the upper Floian through lower Dapingian in the succession including the Köpingsklint and lower Bruddesta formations in the Tingskullen core (*O. evae* and *B. triangularis* zones). This excursion has been well documented in coeval strata from the Siljan area in central Sweden (Lehnert *et al*. 2014), the Precordillera of western Argentina (Buggisch, Keller & Lehnert, 2003) and possibly in North China (Guo

https://doi.org/10.1017/S0016756816000017 Published online by Cambridge University Press

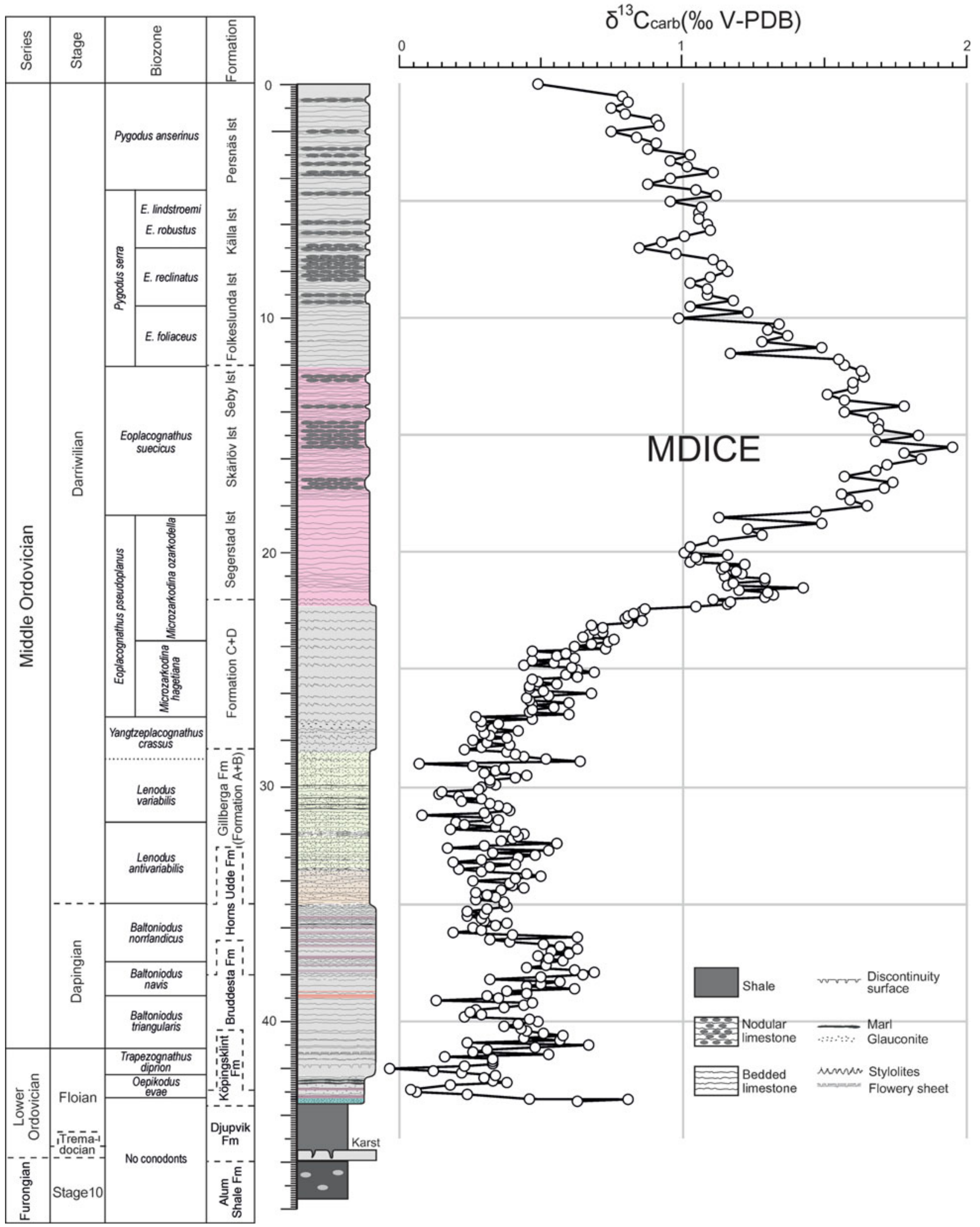

Figure 8. High-resolution $\delta^{13}C$ chemostratigraphy of the Ordovician succession in the Tingskullen drill core from Öland, southeastern Sweden. The Middle Darriwilian Isotope Carbon Excursion (MDICE) is exceptionally well preserved, showing a rising limb through the *Eoplacognathus pseudoplanus* conodont Zone, a distinct peak interval scattering around 1.5–2.0 ‰ in the *Eoplacognathus suecicus* Zone, and a falling limb that corresponds to the *Pygodus serra* and *Pygodus anserinus* conodont zones.

et al. 2014) (Figs 10, 11). Edwards & Saltzman (2014) observed a similar trend in the same stratigraphical interval in the Shingle Pass and Ibex sections in western North America (Fig. 10).

As indicated by a few earlier studies (Kaljo, Martma & Saadre, 2007; Schmitz, Bergström & Wang, 2010; Ainsaar *et al*. 2010; Leslie *et al*. 2011; Albanesi *et al*. 2013) and as further strengthened by our data, the

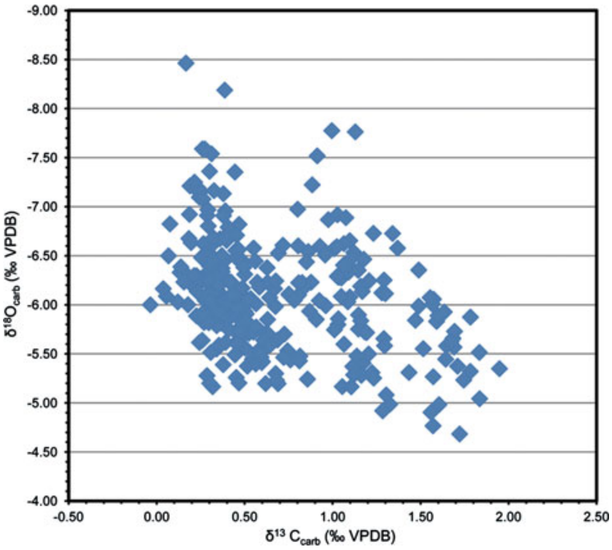

Figure 9. (Colour online) Cross-plot of $\delta^{13}C$ and $\delta^{18}O$ data from the Tingskullen drill core.

MDICE reflects a global anomaly in the global carbon cycle within the Darriwilian and thus is a useful chemostratigraphic marker for global correlation. The tripartite subdivision of the MDICE in the Tingskullen core, showing a rising limb, a peak interval and a falling limb, can be correlated with the BC2, BC3 and part of the BC4 zones of Ainsaar *et al.* (2010), respectively. Schmitz, Bergström & Wang (2010) documented the MDICE from the Hällekis quarry, southern Sweden, and the Maocaopu and Puxi river sections, South China, where only the rising and falling limbs are preserved (Fig. 11). These sections seem to lack the peak interval of the MDICE when compared to the detailed $\delta^{13}C_{carb}$ record from the Tingskullen core. Guo *et al.* (2014) documented one $\delta^{13}C_{carb}$ curve from the Ordos Basin on the North China Palaeoplate, showing one significant excursion with an offset of *c.* 2.5 ‰ within the Klimoli Formation, whose age falls in the Darriwilian, with the conodont *Histiodella kristinae* Zone and the graptolite *Pterograptus elegans* and *Didymograptus murchisoni* zones recorded (Wang *et al.* 2013) (Fig. 10). As such, we suggest that the positive shift in the Klimoli Formation represents the MDICE in the North China Palaeoplate. Furthermore, a Darriwilian $\delta^{13}C_{carb}$ curve was reported from the Precordillera of Argentina (Albanesi *et al.* 2013), where only the rising limb of the MDICE and the probable lower part of the peak interval are observed. The classic curve by Buggisch, Keller & Lehnert (2003) from the same region may only record the rising limb of the MDICE (Fig. 10). In addition, Leslie *et al.* (2011) observed a complete MDICE from the southern Appalachians spanning from the *Histiodella holodentata* to the *Cahabagnathus sweeti* conodont zones, while the peak interval of the MDICE is present in the uppermost *H. holodentata* and *Phragmodus polonicus* zones (Fig. 10). The $\delta^{13}C_{carb}$ record documented by Lehnert *et al.* (2014) from the Mora 001 and Solberga 1 cores clearly shows that the complete MDICE is preserved in the Siljan area of central Sweden (Fig. 11).

5.c. Concluding remarks about the MDICE

This paper does not attempt to explain the cause(s) for the MDICE, but should be seen as a stratigraphic paper providing the necessary data to confirm and further refine the MDICE as a global phenomenon useful for regional and intercontinental correlations. The Tingskullen core should be useful for continued study about the MDICE, and a few concluding remarks to put the MDICE in a wider context are necessary.

A series of studies now imply that the MDICE is of global significance, meaning that global processes account for its formation. Increased sequestration and burial of ^{12}C started in the *E. pseudoplanus* Zone (or even in the *Y. crassus* Zone) and reached a maximum during the *E. suecicus* Zone before the process reversed. This global perturbation in the ocean–atmosphere system is of particular importance because it overlaps in time with important segments of one of the largest biodiversification events of the Phanerozoic: the Great Ordovician Biodiversification Event (GOBE; Webby *et al.* 2004; Harper, 2006; Servais *et al.* 2010). During the GOBE the marine biodiversity tripled at the family, genus and species levels, and it has been demonstrated that the increase in biodiversity was especially profound in the Darriwilian Age (Webby *et al.* 2004; Harper, 2006) corresponding in time with the MDICE. The cause for this major advance of marine life is debated and direct causal relationships remain unexplained. Among the proposed explanations are cooling of the global oceans following the demise of the Early–Mid Ordovician greenhouse world (Trotter *et al.* 2008), biological triggers such as increased levels of phytoplankton and primary production in the global oceans (Servais *et al.* 2008) and extraterrestrial forcing mechanisms (Schmitz *et al.* 2008). Furthermore, it is worthy to note that acritarchs, possibly representing the marine primary productivity, reached their major biodiversity peak during Darriwilian time (Servais *et al.* 2008). Thus, we suggest that the increased primary productivity, induced by the concurrent phytoplankton (e.g. acritarch) diversification during Darriwilian time, may play an important role in the development of the MDICE.

6. Conclusions

Based on the cool-water carbonate succession ('orthoceratite limestone') of the Tingskullen core from Öland, southeastern Sweden, this study presents a high-resolution, integrated conodont biostratigraphy and carbon isotope chemostratigraphy for the Lower–Middle Ordovician of southern Sweden.

The major results can be concluded as follows:

(1) Based on the analysis of conodonts, the carbonate succession in the Tingskullen core ranges from

https://doi.org/10.1017/S0016756816000017 Published online by Cambridge University Press

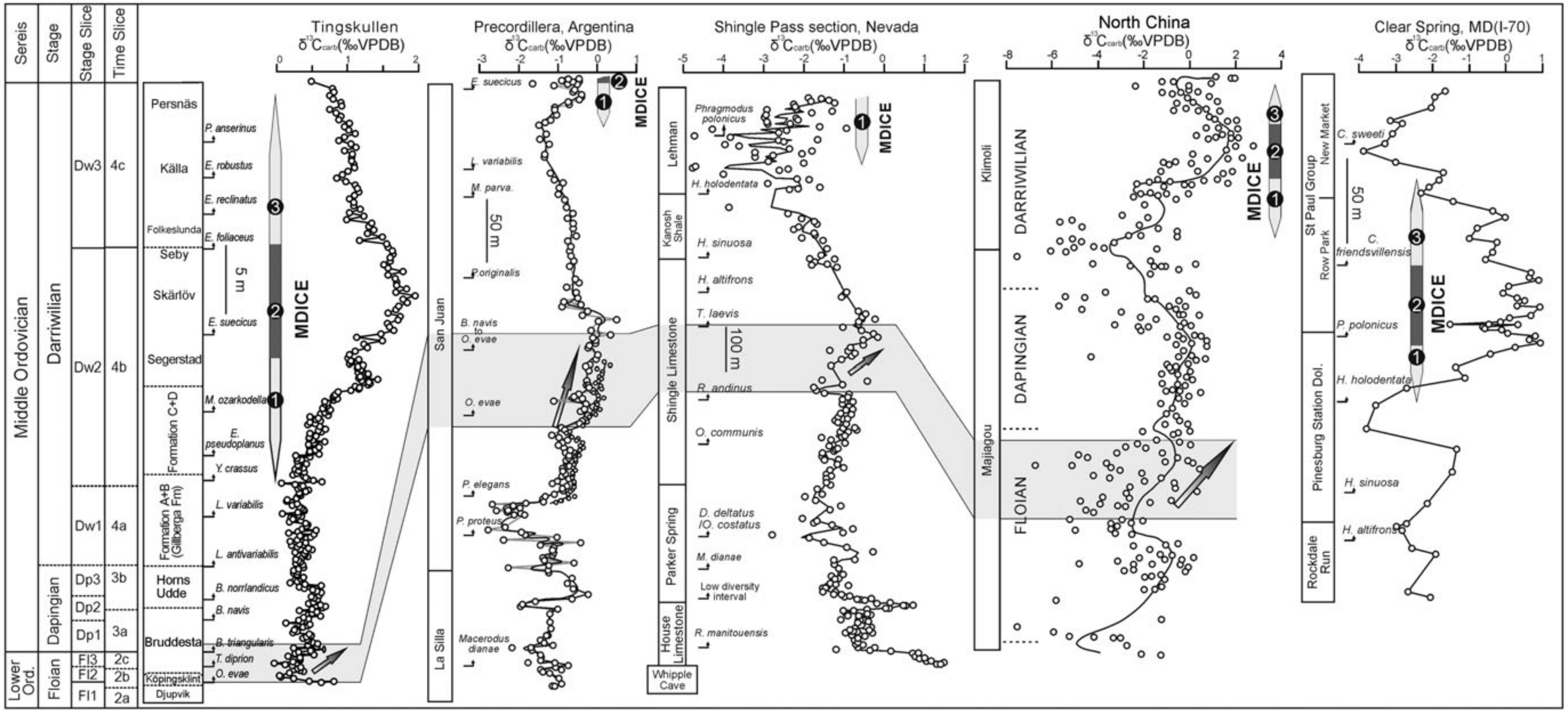

Figure 10. Comparison of the $\delta^{13}C$ records from the Tingskullen core (this study), Precordillera (Buggisch, Keller & Lehnert, 2003), Nevada, USA (Edwards & Saltzman, 2014), Maryland, USA (Leslie *et al.* 2011) and North China (Guo *et al.* 2014). The numbers 1–3 in the $\delta^{13}C$ record from the Tingskullen core refer to the rising limb, the peak interval and the falling limb of the MDICE, respectively. Note the very high condensation of strata in the Tingskullen core, as indicated by scale bars.

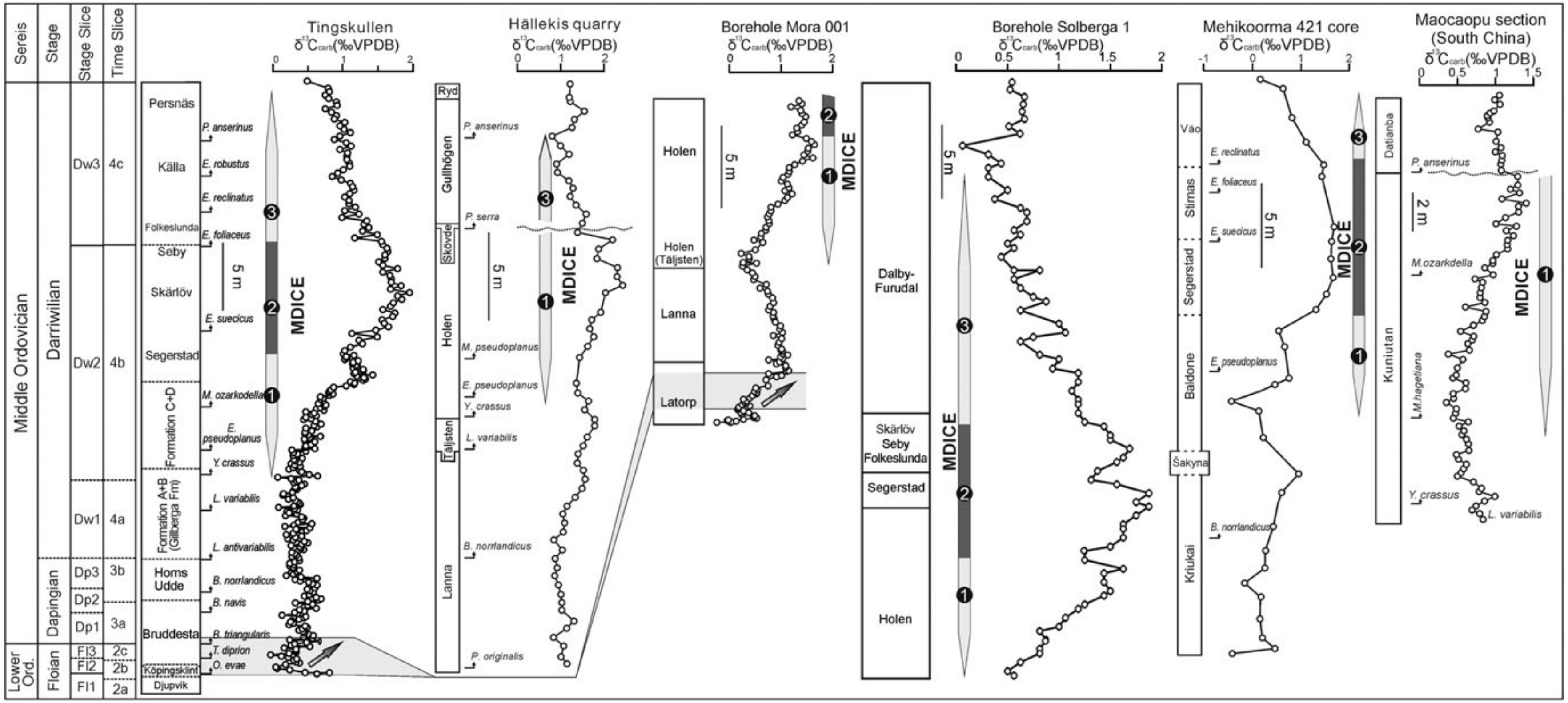

Figure 11. Comparison of the $\delta^{13}C$ records from the Tingskullen core (this study), Hällekis quarry of southern Sweden (Schmitz, Bergström & Wang, 2010), Mora 001 and Solberga 1 cores from the Siljan area of central Sweden (Lehnert *et al*. 2014), Mehikoorma 421 core of Estonia (Ainsaar *et al*. 2010) and South China (Schmitz, Bergström & Wang, 2010). The numbers 1–3 in the $\delta^{13}C$ record from the Tingskullen core refer to the rising limb, the peak interval and the falling limb of the MDICE, respectively.

the *Oepikodus evae* Zone through *Pygodus anserinus* Zone.

(2) The lower part of the core, including the succession from the Köpingsklint Formation through Gillberga Formation (Formation A + B), is characterized by only little variation in $\delta^{13}C_{carb}$ values. One positive excursion, however, with high potential for global correlation can be observed spanning the upper Köpingsklint and lower Bruddesta formations, an interval corresponding to the upper *O. evae* Zone and lower *B. triangularis* Zone.

(3) The Tingskullen core preserves one of the few and most complete records of the MDICE globally. This $\delta^{13}C_{carb}$ anomaly appears to be exceptionally well preserved and shows a rising limb in the *E. pseudoplanus* Zone, ranging from Formation C + D through most of the Segerstad Limestone, a peak interval (peak value 1.95 ‰) in the *E. suecicus* Zone, in the upper Segerstad, Skärlöv and Seby limestones, and a falling limb during the *P. serra* and *P. anserinus* zones, corresponding to the Folkeslunda, Källa and Persnäs limestones. Correlation is made to several other basins.

(4) The development of the MDICE is likely related to an increase in organic carbon burial rates as a result of a synchronous enhanced primary productivity, which may be indirectly extrapolated by the radiation of phytoplankton and diversification in major faunal groups. The cause for this radiation remains debated.

Acknowledgements. RCW and MC acknowledge the support by the Swedish Research Council. Crafoord Foundation grants 20050748 and 20080860 to MC made the recovery of the Borenshult and Tingskullen drill cores, respectively, possible. OL is very grateful for the support of this research by the Deutsche Forschungsgemeinschaft (DFG project LE 867/8-1 and 8-2). RCW acknowledges the support from the National Natural Science Foundation of China (41521061 and 41290260). We thank Prof. Michael Joachimski for excellent help with running the carbon isotope samples in his stable isotope laboratory at the Geocentre of Northern Bavaria in Erlangen (Germany). We acknowledge Prof. Birger Schmitz (Lund University) and one anonymous referee for their comments that have improved our manuscript. This paper is a contribution to the IGCP 591 project 'The Early to Middle Paleozoic Revolution'.

References

AINSAAR, L., KALJO, D., MARTMA, T., MEIDLA, T., MÄNNIK, P., NÕLVAK, J. & TINN, O. 2010. Middle and Upper Ordovician carbon isotope chemostratigraphy in Baltoscandia: a correlation tool and clues to environmental history. *Palaeogeography, Palaeoclimatology, Palaeoecology* **294**, 189–201.

AINSAAR, T., MEIDLA, T. & MARTMA, T. 1999. Evidence for a widespread carbon isotopic event associated with late Middle Ordovician sedimentological and faunal changes in Estonia. *Geological Magazine* **136**, 49–62.

AINSAAR, L., MEIDLA, T. & TINN, O. 2004. Middle and Upper Ordovician stable isotope stratigraphy across the facies belts in the East Baltic. In *WOGOGOB-2004: Conference Materials* (eds O. Hints & L. Ainsaar), pp. 11–12. Tartu: Tartu University Press.

AINSAAR, L., MEIDLA, T., TINN, O., MARTMA, T. & DRONOV, A. 2007. Darriwilian (Middle Ordovician) carbon isotope stratigraphy in Baltoscandia. *Acta Palaeontologica Sinica* **46**(Suppl.), 1–8.

ALBANESI, G. L., BERGSTRÖM, S. M., SCHMITZ, B., SERRA, F., FELTES, N. A., VOLDMAN, G. G. & ORTEGA, G. 2013. Darriwilian (Middle Ordovician) $\delta^{13}C_{carb}$ chemostratigraphy in the Precordillera of Argentina: documentation of the middle Darriwilian Isotope Carbon Excursion (MDICE) and its use for intercontinental correlation. *Palaeogeography, Palaeoclimatology, Palaeoecology* **389**, 48–63.

AN, T. X. 1981. Recent progress in Cambrian and Ordovician conodont biostratigraphy of China. *Geological Society of America Special Paper* **187**, 209–17.

AN, T. X.1987. *Early Paleozoic Conodonts from South China*. Beijing: Peking University Publishing House, 238 pp. (in Chinese).

AZMY, K., STOUGE, S., CHRISTIANSEN, J. L., HARPER, D. A. T., KNIGHT, I. & BOYCE, D. 2010. Carbon-isotope stratigraphy of the Lower Ordovician succession in Northeast Greenland: implications for correlations with St. George Group in western Newfoundland (Canada) and beyond. *Sedimentary Geology* **225**, 67–81.

BAGNOLI, G. & STOUGE, S. 1997. Lower Ordovician (Billingenian – Kunda) conodont zonation and provinces based on sections from Horns Udde, north Öland, Sweden. *Bullettino della Societa Paleontologica Italiana* **35**, 109–63.

BANNER, J. L. & HANSON, G. N. 1990. Calculation of simultaneous isotopic and trace element variations during water interaction with applications to carbonate diagenesis. *Geochimica et Cosmochimica Acta* **54**, 3123–37.

BERGSTRÖM, S. M. 1971. Conodont biostratigraphy of the Middle and Upper Ordovician of Europe and Eastern North America. *Geological Society of America Memoir* **127**, 83–161.

BERGSTRÖM, S. M., CALNER, M., LEHNERT, O. & NOOR, A. 2011. A new upper Middle Ordovician–Lower Silurian drillcore standard succession from Borenshult in Östergötland, southern Sweden: 1. Stratigraphical review with regional comparisons. *GFF* **133**, 149–71.

BERGSTRÖM, S. M., CHEN, X., GUTIÉRREZ-MARCO, J. C. & DRONOV, A. 2009. The new chronostratigraphic classification of the Ordovician System and its relations to major regional series and stages and to $\delta^{13}C$ chemostratigraphy. *Lethaia* **42**, 97–107.

BERGSTRÖM, S. M., LEHNERT, O., CALNER, M. & JOACHIMSKI, M. M. 2012. A new upper Middle Ordovician–Lower Silurian drillcore standard succession from Borenshult in Östergötland, southern Sweden: 2. Significance of $\delta^{13}C$ chemostratigraphy. *GFF* **134**, 39–63.

BERGSTRÖM, J., PÄRNASTE, H. & ZHOU, Z. Y. 2013. Trilobites and biofacies in the Early–Middle Ordovician of Baltica and a brief comparison with the Yangtze Plate. *Estonian Journal of Earth Sciences* **62**(4), 205–30.

BRENCHLEY, P. J., CARDEN, G. A., HINTS, L., KALJO, D., MARSHALL, J. D., MARTMA, T., MEIDLA, T. & NÕLVAK, J. 2003. High-resolution stable isotope stratigraphy of Upper Ordovician sequences: constraints on the timing of bioevents and environmental changes associated with mass extinction and glaciation. *Geological Society of America Bulletin* **115**, 89–104.

BUGGISCH, W., KELLER, M. & LEHNERT, O. 2003. Carbon isotope record of the Late Cambrian and Early Ordovician carbonates of the Argentine Precordillera. *Palaeogeography, Palaeoclimatology, Palaeoecology* **195**, 357–73.

CALNER, M., LEHNERT, O., WU, R. C., DAHLQVIST, P. & JOACHIMSKI, M. M. 2014. $\delta^{13}C$ chemostratigraphy in the Lower–Middle Ordovician succession of Öland (Sweden) and the global significance of the MDICE. *GFF* **136**, 48–54.

EDWARDS, C. T. & SALTZMAN, M. R. 2014. Carbon isotope ($\delta^{13}C_{carb}$) stratigraphy of the Lower–Middle Ordovician (Tremadocian–Darriwilian) in the Great Basin, western United States: implications for global correlation. *Palaeogeography, Palaeoclimatology, Palaeoecology* **399**, 1–20.

EPSTEIN, A. G., EPSTEIN, J. B. & HARRIS, L. D.1977. Conodont color alteration – an index to organic metamorphism. *US Geological Survey Professional Paper* **995**, 1–27.

GUO, Y. R., ZHAO, Z. Y., XU, W. Y., SHI, X. Y., GAO, J. R., BAO, H. P., LIU, J. B., ZHANG, Y. L. & ZHANG, Y. Q.2014. Sequence stratigraphy of the Ordovician System in the Ordos Basin. *Acta Sedimentologica Sinica* **32**(1), 44–60 (in Chinese with English abstract).

HARPER, D. A. T. 2006. The Ordovician biodiversification: setting an agenda for marine life. *Palaeogeography, Palaeoclimatology, Palaeoecology* **232**, 148–66.

JAANUSSON, V. 1960. The Viruan (Middle Ordovician) of Öland. *Publications from the Palaeontological Institution of the University of Uppsala* **28**, 207–88. (Reprinted from: *The Bulletin of the Geological Institutions of the University of Uppsala* Vol. XXXVIII).

JAANUSSON, V. 1961. Discontinuity surfaces in limestones. *Publications from the Palaeontological Institution of the University of Uppsala* **35**, 221–41. (Reprinted from: *The Bulletin of the Geological Institutions of the University of Uppsala* Vol. XL).

JAANUSSON, V. 1976. Faunal dynamics in the Middle Ordovician (Viruan) of Baltoscandia. In *The Ordovician System* (ed. M. G. Bassett), pp. 301–26. Cardiff: University of Wales Press and National Museum of Wales.

JAANUSSON, V. 1982. Introduction to the Ordovician of Sweden. In *Field Excursion Guide. 4th International Symposium on the Ordovician System* (eds D. L. Bruton & S. H. Williams), pp. 1–10. Paleontological Contributions from the University of Oslo 279.

JAANUSSON, V. 1995. Confacies differentiation and upper Middle Ordovician correlation in the Baltoscandian basin. *Proceedings of the Estonian Academy of Science, Geology* **44**, 73–86.

JEPPSSON, L., ANEHUS, R. & FREDHOLM, D. 1999. The optimal acetate buffered acetic acid technique for extracting phosphatic fossils. *Journal of Paleontology* **73**, 964–72.

KALJO, D., MARTMA, T. & SAADRE, T. 2007. Post-Hunnebergian Ordovician carbon isotope trend in Baltoscandia, its environmental implications and some similarities with that of Nevada. *Palaeogeography, Palaeoclimatology, Palaeoecology* **245**, 138–55.

LEHNERT, O., MEINHOLD, G., WU, R. C., CALNER, M. & JOACHIMSKI, M. M. 2014. $\delta^{13}C$ chemostratigraphy in the upper Tremadocian through lower Katian (Ordovician) carbonate succession of the Siljan district, central Sweden. *Estonian Journal of Earth Sciences* **63**(4), 277–86.

LESLIE, S. A., SALTZMAN, M. R., BERGSTRÖM, S. M., REPETSKI, J. E., HOWARD, A. & SEWARD, A. M.2011. Conodont biostratigraphy and stable isotope stratigraphy across the Ordovician Knox/Beekmantown unconformity in the central Appalachians. In *Ordovician of the World* (eds J. C. Gutiérrez-Marco, I. Rábano & G.-B. Diego), pp. 301–8. Publicaciones del Instituto Geológico y Minero de España, Serie, Cuadernos del Museo Geomin-Minero Vol. 14.

LI, Z. H., STOUGE, S., CHEN, X. H., WANG, C. S., WANG, X. F. & ZENG, Q. L. 2010. Precisely compartmentalized and correlated Lower Ordovician *Oepikodus evae* Zone of the Floian in the Huanghuachang Section, Yichang, Hubei Province. *Acta Palaeontologica Sinica* **49**, 108–24 (in Chinese with English abstract).

LINDSTRÖM, M. 1971. Lower Ordovician conodonts of Europe. *Geological Society of America Memoir* **127**, 21–61.

LÖFGREN, A. 1978. Arenigian and Llanvirnian conodonts from Jämtland, northern Sweden. *Fossils and Strata* **19**, 1–129.

LÖFGREN, A. 1994. Arenig (Lower Ordovician) conodonts and biozonation in the eastern Siljan District, central Sweden. *Journal of Paleontology* **68**, 1350–68.

LÖFGREN, A. 2000. Early to early Middle Ordovician conodont biostratigraphy of the Gillberga quarry, northern Öland, Sweden. *GFF* **122**, 321–38.

LÖFGREN, A. 2003. Conodont faunas with *Lenodus variabilis* in the upper Arenigian to lower Llanvirnian of Sweden. *Acta Palaeontologica Polonica* **48**, 417–36.

LUDVIGSON, G. A., JACOBSON, S. R., WITZKE, B. J. & GONZÁLEZ, L. A. 1996. Carbonate component chemostratigraphy and depositional history of the Ordovician Decorah Formation, Upper Mississippi Valley. *Geological Society of America Special Paper* **306**, 67–86.

LUDVIGSON, G. A., WITZKE, B. J., SCHNEIDER, C. L., SMITH, E. A., EMERSON, N. R., CARPENTER, S. J. & GONZÁLEZ, L. A. 2004. Late Ordovician (Turonian – Chatfieldian) carbon isotope excursions and their stratigraphic and paleoceanic significance. *Palaeogeography, Palaeoclimatology, Palaeoecology* **210**, 187–214.

MARSHALL, J. D. 1992. Climatic and oceanographic isotopic signals from the carbonate rock record and their preservation. *Geological Magazine* **129**, 143–60.

MEIDLA, T., AINSAAR, L., BACKMAN, J., DRONOV, A., HOLMER, L. & STURESSON, U. 2004. Middle–Upper Ordovician carbon isotope record from Västergötland (Sweden) and East Baltic. In *WOGOGOB-2004 Conference Materials* (eds O. Hints & L. Ainsaar), pp. 67–8. Tartu: Tartu University Press.

MUNNECKE, A., ZHANG, Y. D., LIU, X. & CHENG, J. F. 2011. Stable carbon isotope stratigraphy in the Ordovician of South China. *Palaeogeography, Palaeoclimatology, Palaeoecology* **307**, 17–43.

PÄRNASTE, H., BERGSTRÖM, J. & ZHOU, Z. Y. 2013. High resolution trilobite stratigraphy of the Lower–Middle Ordovician Öland Series of Baltoscandia. *Geological Magazine* **150**, 509–18.

PATZKOWSKY, M. E., SLUPIK, L. M., ARTHUR, M. A., PANCOST, R. D. & FREEMAN, K. H.1997. Late Middle Ordovician environmental change and extinction: harbinger of the Late Ordovician or continuation of Cambrian patterns? *Geology* **25**, 911–4.

SALTZMAN, M. R. 2005. Phosphorus, nitrogen, and the redox evolution of the Paleozoic oceans. *Geology* **33**, 573–6.

SALTZMAN, M. R. & YOUNG, S. A. 2005. Long-lived glaciation in the Late Ordovician? Isotopic and sequence-stratigraphic evidence from western Laurentia. *Geology* **33**, 109–12.

SCHMITZ, B., BERGSTRÖM, S. M. & WANG, X. F. 2010. The middle Darriwilian (Ordovician) $\delta^{13}C$ excursion (MDICE) discovered in the Yangtze Platform succession in China: implications of its first recorded occurrences outside Baltoscandia. *Journal of the Geological Society, London* **167**, 249–59.

Schmitz, B., Harper, D. A. T., Peucker-Ehrenbrink, B., Stouge, S., Alwmark, C., Chronholm, A., Bergström, S. M., Tassinari, M. & Wang, X. F.2008. Asteroid breakup linked to the Great Ordovician Biodiversification Event. *Nature Geoscience* **1**, 49–53.

Serpagli, E.1974. Lower Ordovician conodonts from Precordilleran Argentina (Province of San Juan). *Bollettino della Società Paleontologica Italiana* **13**, 17–98.

Servais, T., Lehnert, O., Li, J., Mullins, G. L., Munnecke, A., Nützel, A. & Vecoli, M. 2008. The Ordovician Biodiversification: revolution in the oceanic trophic chain. *Lethaia* **41**, 99–109.

Servais, T., Owen, A. W., Harper, D. A. T., Kröger, B. & Munnecke, A. 2010. The Great Ordovician Biodiversification Event (GOBE): the palaeoecological dimension. *Palaeogeography, Palaeoclimatology, Palaeoecology* **294**, 99–119.

Stouge, S. 2004. Ordovician siliciclastics and carbonates of Öland, Sweden. In *International Symposium on "Early Palaeozoic Palaeogeography and Palaeolimate" (IGCP 503), September 1–3, 2004, Erlangen, Germany* (eds A. Munnecke, T. Servais & C. Schulbert), pp. 91–111. Erlanger Geologische Abhandlungen – Sonderband 5.

Stouge, S. & Bagnoli, G. 1988. Early Ordovician conodonts from Cow Head Peninsula, western Newfoundland. *Palaeontographica Italica* **75**, 89–179.

Tjernvik, T. 1952. Om de lägsta ordoviciska lagren i Närke. *Geologiska Föreningens I Stockholm Förhandlingar* **74**, 51–70.

Tjernvik, T. 1956. On the Early Ordovician of Sweden. Stratigraphy and fauna. *Bulletin of the Geological Institutions of the University of Uppsala* **36**, 107–284.

Torsvik, T. H., Smethurst, M. A., Van der Voo, R., Trench, A., Abrahamsen, N. & Halvorsen, E.1992. Baltica. A synopsis of Vendian–Permian palaeomagnetic data and their palaeotectonic implications. *Earth-Science Reviews* **33**, 133–52.

Trotter, J. A., Williams, I. S., Barnes, C. R., Lécuyer, C. & Nicoll, R. S. 2008. Did cooling oceans trigger Ordovician biodiversification? Evidence from conodont thermometry. *Science* **321**, 550–4.

van Wamel, W. A. 1974. Conodont biostratigraphy of the Upper Cambrian and Lower Ordovician of north-western Öland, southeastern Sweden. *Utrecht Micropaleontological Bulletins* **10**, 1–126.

Viira, V. 1974. *Konodonty Ordovika Pribaltiki [Ordovician Conodonts of the East Baltic]*. Tallinn: Valgus, 142 pp.

Wang, Z. H. & Bergström, S. M.1999. Conodonts across the base of the Darriwilian Stage in South China. *Acta Micropalaeontologica Sinica* **16**, 325–50 (in Chinese with English abstract).

Wang, Z. H., Bergström, S. M., Zhen, Y. Y., Chen, X. & Zhang, Y. D.2013. On the integration of Ordovician conodont and graptolite biostratigraphy: new examples from Gansu and Inner Mongolia in China. *Alcheringa* **37**, 510–28.

Wang, X. F., Stouge, S., Chen, X. H., Li, Z. H., Wang, C. S., Finney, S. C., Zeng, Q. L., Chen, H. M. & Erdtmann, E.-D. 2009. The global stratotype section and point for the base of the Middle Ordovician series and the third stage (Dapingian). *Episodes* **32**, 96–113.

Wang, X. F., Stouge, S., Erdtmann, B.-D., Chen, X. H., Li, Z. H., Wang, C. S., Zeng, Q. L., Zhou, Z. Q. & Cheng, H. M.2005. A proposed GSSP for the base of the Middle Ordovician Series: the Huanghuachang section, Yichang, China. *Episodes* **28**, 105–17.

Webby, B. D., Droser, M. L., Paris, F. & Percival, I. G. (eds) 2004. *The Great Ordovician Biodiversification Event*. New York: Columbia University Press, 484 pp.

Westergård, A. H. 1922. Sveriges olenidskiffer. – I. Utbredning och Lagerföljd. II. Fauna 1. Trilobita. *Sveriges Geolologiska Undersökning Series Ca* **18**, 205 pp.

Young, S. A., Saltzman, M. R. & Bergström, S. M. 2005. Upper Ordovician (Mohawkian) carbon isotope ($\delta^{13}C$) stratigraphy in eastern and central North America: regional expression of a perturbation of the global carbon cycle. *Palaeogeography, Palaeoclimatology, Palaeoecology* **222**, 53–76.

Zhang, J. H. 1998a. Middle Ordovician conodonts from the Atlantic Faunal Region and the evolution of key conodont genera. *Meddelanden från Stockholms Universitets institution för Geologi Och Geokemi* **298**, 5–27.

Zhang, J. H. 1998b. Conodonts from the Guniutan Formation (Llanvirnian) in Hubei and Hunan Provinces, south-central China. *Stockholm Contributions in Geology* **46**, 1–161.

Zhang, Y. D., Munnecke, A., Chen, X., Cheng, J. F. & Liu, X. 2011. Biostratigraphic and chemostratigraphic correlation for the base of the Middle Ordovician between Yichang and western Zhejiang areas, South China. *Acta Geologica Sinica* **85**, 320–9.

Zhang, J. H. & Sturkell, E. F. F. 1998. Aserian and Lasnamägian (Middle Ordovician) conodont biostratigraphy and lithology at Kullstaberg and Lunne in Jämtland, central Sweden. *GFF* **120**, 75–83.